FEASIBILITY STUDY OF NON-CONTACT MONITORING OF HEART RATE USING A CAPACITIVELY COUPLED SCHEME INTEGRATED INTO THE SEATBELT OF A CAR

A THESIS

Submitted by

KALLAKURI GURUCHARAN TEJA

(EE12M106)

For the award of the degree

Of

MASTER OF TECHNOLOGY

DEPARTMENT OF ELECTRICAL ENGINEERING

INDIAN INSTITUTE OF TECHNOLOGY MADRAS

MAY 2014

THESIS CERTIFICATE

This is to certify that the thesis titled **FEASIBILITY STUDY OF NON-CONTACT MONITORING OF HEART RATE USING A CAPACITIVELY COUPLED SCHEME INTEGRATED INTO THE SEAT BELT,** submitted by **KALLAKURI GURUCHARAN TEJA**, to the Indian Institute of Technology Madras, Chennai in partial fulfilment of the requirements for the award of the degree of **Master of Technology** (Control & Instrumentation) in Electrical Engineering, is a bona fide record of the research work done by him under my supervision and guidance. The contents of this project thesis, in full or in parts have not been submitted to any other university/institute for the award of any degree or diploma.

Dr. Boby George

Project guide

Assistant Professor

Dept. of Electrical Engineering

IIT Madras, 600036

Place: Chennai

Date: 16th May 2014

ACKNOWLEDGEMENTS

I wish to express my sincere gratitude for my guide Dr. Boby George, Department of Electrical Engineering, IIT Madras, for his invaluable support guidance and attention throughout the entire period of project work. His kind nature in providing all the necessary facilities for the successful completion of this project work, is earnestly acknowledged.

I would like to thank all the volunteers- Sridhar, Devi Prasad, Aniketh Anil More, Danish, Sarath, Anish Babu, for their consent to have HRV analysis performed using their HRV data which enabled me to document the results. Special thanks go out to my seniors and friends Mr Anoop CS and Mr Biswaroop for their timely advice on any query I may have had regarding my project work. I would like to express my gratitude towards Mr Pillai, Measurement and Instrumentation Lab, Dept. of Electrical Engineering, IIT Madras for constantly striving to ensure the availability of all the components necessary for the smooth completion of a project work.

With a sense of deep gratitude, I acknowledge the support my family has offered whenever I needed it.

GURUCHARAN TEJA. K.

ABSTRACT

KEYWORDS: Non-contact electrocardiography, capacitive coupling, active shielding, novel ECG electrodes, HRV analysis, car's seat belt virtual instrument.

The ECG is a very important, non-invasive marker of cardiac activity. It provides vital information of the cardiovascular functioning in a patient. The conventional ECG instrument requires direct contact between the electrodes and the patient's skin. The present non-contact electrocardiography scheme requires no such direct contact with the patient's skin which is why it is preferred to the conventional ECG recording instruments especially while recording the ECG of an infant or a premature baby, from the elderly patients and from those whose skin is sensitive to gel-irritation. There has been growing interest in the cardiovascular monitoring inside a car. Research has been going on in this direction because the drivers are vulnerable to cardiac arrests and their monitoring is very important. Furthermore, Heart rate is also an unequivocal indicator of drowsiness of the driver. Previous schemes have suggested the use of the non-contact scheme in the back of a car's seat. This present scheme incorporates ECG recording from the electrodes placed in the seat belt of a car.

The proposed non-contact scheme presented in this thesis is based on sensing the variations in the electric potential close to the patient's relevant body surface. This method doesn't use any conductive gel unlike in conventional ECG measurements, where the surface electrodes are pasted on chest or limbs and the signal is acquired via Ag/Agcl conductive gel. In order to measure the potential, suitable capacitive electrodes are designed and developed. These electrodes are placed few mm away from the skin surface. These plates and the electric signal source inside the body forms a capacitive coupling and the electric bio-signal can be derived through this non-contact electrode. The clothing and the skin perform the function of a dielectric medium.

A prototype has been built, tested and non-contact ECG signals have been acquired from many volunteers and the same was verified with their conventional ECG. It has been noticed that the developed non-contact scheme provides reliable and very good signal quality without losing any important morphological information just like the conventional ECG scheme.

The scheme presented in this thesis incorporated non-contact ECG from the car's seat belt. Due to changes in demographics and an increase in the number of elderly car-drivers, medical-assistance systems in the automotive environment are gaining importance. In this system, two actively shielded electrodes placed in the shoulder harness (sash belt) are used to measure the bio-potentials with respect to the reference electrode placed in the lap belt using capacitive sensing method. The signal acquired from the active electrodes are amplified using an instrumentation amplifier and filtered. This signal is next digitized using a National Instruments MyDAQ data acquisition system and displayed on a Virtual Instrument developed using LabVIEW environment. Any other necessary filtering is done using LabVIEW. Heart rate signal or the RR tachogram is extracted from the ECG signal and used to perform the heart rate variability (HRV) analysis. The present work also demonstrates different methods to quantify HRV.

TABLE OF CONTENTS

ACKNOWLEDGEMENTS i

ABSTRACT ii

LIST OF TABLES vii

LIST OF FIGURES vi

ABBREVIATIONS viii

CHAPTER 1: INTRODUCTION…… 1

1.1 Electrocardiography……1

1.2 The cardiac conduction system……...2

1.3 The Electrocardiogram……3

1.3.1 The origin of ECG……...3

1.4 Objective and scope of the project……..5

1.5 Organization of the thesis……6

CHAPTER 2: EXISTING NONCONTACT HR MEASUREMENT TECHNIQUES……7

2.1 Drawbacks of existing ECG measurement schemes……...7

2.2 Noncontact HR measurement schemes……...7

2.2.1 Indirect HR Measurement Based on Doppler Effect……...7

2.2.2 Indirect Methods for HR Measurement Based on Audio……..10

2.2.3 Direct Methods for HR Measurement (cECG)……..11

CHAPTER 3: HEART-RATE VARIABILITY……..14

3.1 Introduction……...14

3.1.1 Background……...14

3.2 Quantifying HRV……..15

3.2.1 Geometric methods……...16

3.2.2 Statistical Indices…….17

3.2.3 Frequency domain methods…….18

3.2.3.1 Power Spectral Analysis……..19

3.2.3.1.1 LF/HF ratio and the sympathovagal balance……...21

3.2.4 Non-linear methods…….22

CHAPTER 4: NON-CONTACT ECG INCORPORATED IN THE CAR'S SEATBELT……...24

4.1 Introduction…….24

4.1.1 Motivation……...25

4.2 Electrode configurations…….26

4.2.1 Electrode configuration 1……....26

4.2.2 Electrode configuration 2……27

CHAPTER 5: VIRTUAL INSTRUMENTATION AND EXPERIMENTAL RESULTS…….31

5.1 Acquisition……..31

5.2 Virtual instrumentation……...33

5.3 Time domain HRV calculations……..38

5.3.1 Algorithm and flowchart for Time domain HRV calculations…….. 40

5.4 Geometric and nonlinear HRV methods…… 42

5.5 Frequency domain HRV measurement…….. 43

5.6 Results…… 44

5.7 Conclusions……50

CHAPTER 6: CONCLUSIONS…….51

6.1 Summary of the work…….51

6.2 Future scope……52

REFERENCES…….53

CURRICULUM VITAE…….55

LIST OF FIGURES

Fig. 1.1: Action potential of a cell…….....1

Fig. 1.2: The cardiac conduction system……2

Fig. 1.3: Typical Electrocardiograph……..3

Fig. 1.4: Superposition of action potentials at various nodes……4

Fig. 2.1: HR measurement using Doppler-effect……...8

Fig. 2.2: Microwave Radar HR measuring device……9

Fig. 2.3: Microwave Radar sensor output vis-à-vis original ECG..…….……10

Fig. 2.4: Ubiquitous health care in the chair and bed……...12

Fig. 2.5: Capacitive ECG in the toilet seat……...12

Fig. 2.6: Noncontact ECG in the car……13

Fig. 3.1: A typical RR tachogram……15

Fig. 3.2: A typical RR interval Histogram……...16

Fig. 3.3: Plot of SDNN vs. Age……....18

Fig. 3.4: Plot of RMSSD, pNN50 vs. Age……...18

Fig. 3.5: FFT spectrum derived from RR tachogram……...19

Fig. 3.6: A typical PSD graph using the AR technique……....20

Fig. 3.7: LF/HF during rest and tilting……21

Fig. 3.8: Autonomous nervous system's impact on HR……...22

Fig. 3.9: A typical Poincaré plot……..22

Fig. 4:1: A typical 3-point BIS configuration……..24

Fig. 4.2: Electric field distribution along the human torso and the corresponding electrodes.25

Fig. 4.3: Seat belt with electrodes prototype……....26

Fig. 4.4: ECG when the slider was positioned at the centre of the chest……26

Fig. 4.5: ECG when the slider was positioned slightly to the left of the chest's centre……...27

Fig 4.6: ECG when the slider was moved slightly to the right……....27

Fig. 4.7: Electrodes and respective shields in the seatbelt……...28

Fig. 4.8: Electrodes and shields along with the seatbelt……...29

Fig. 4.9: A subject wearing a single layered shirt (T-shirt) whose ECG is being recorded….29

Fig. 4.10: Block diagram highlighting the entire acquisition procedure..……30
Fig. 5.1: NI myDAQ……31
Fig. 5.2: Signal processing and signal acquisition unit……32
Fig. 5.3: Functional block diagram……..32
Fig. 5.4: Experimental setup……33
Fig. 5.5: Block diagram developed to perform HRV……...35
Fig 5.6: Baseline wandering removal in ECG……..37
Fig. 5.7: VI for RR interval calculation……38
Fig. 5.8: VI for time domain HRV indices calculation……....39
Fig. 5.9: VI for Geometrical methods of HRV……42
Fig. 5.10: VI for calculation of HRV indices using Poincaré plot……..42
Fig. 5.11: Block diagram highlighting FFT HRV method……..43
Fig. 5.12: Volunteer with the seat belt setup……...44
Fig. 5.13: ECG and RR tachogram of a 23 year old subject……...44
Fig. 5.14: Statistical HRV analysis……45
Fig. 5.15: BPM variations in the 23 year old male subject……45
Fig.5.16: AR power spectral density……...46
Fig.5.17: FFT HR spectrum……46
Fig. 5.18: Poincaré plot analysis in 23 year old subject……..46
Fig. 5.19: ECG and RR tachogram of the 35 year old subject……47
Fig. 5.20: Statistical HRV components of the 35y/o subject……..47
Fig. 5.21: BPM variations in the 35 y/o subject……48
Fig. 5.22: HR (BPM) variations……48

LIST OF TABLES

Table 5.1: HRV indices of all the volunteers……45

ABBREVIATIONS

ECG – Electrocardiogram

RA – Right Atrium

RV – Right Ventricle

LA – Left Atrium

LV – Left Ventricle

SA – Sino-Atrial

Bpm – Beats per minute

INA – Instrumentation Amplifier

HPF – High Pass Filter

BPF – Band Pass Filter

VI – Virtual Instrument

LabVIEW - Laboratory Virtual Instrumentation Engineering Workbench

HRV – Heart Rate Variability

LF – Low Frequency

HF – High Frequency

SIDS – Sudden Infant Death Syndrome

HR – Heart Rate

DAQ – Data Acquisition System

US – Ultrasound

Rpm – Respirations per minute

PSD – Power Spectral Density

cECG – Capacitive ECG

CHAPTER 1

INTRODUCTION

1.1 Electrocardiography

ECG- Electrocardiograph is a major diagnostic tool for the assessment of the health of the heart. It is the most commonly known and recognized biomedical signal. ECG is the electrical manifestation of the contractile activity of the heart and can be recorded fairly easily with surface electrodes on the limbs or chest. Cells in humans act like little batteries. These cells have different ion concentrations inside and outside of their membranes which create small electric potentials called biopotentials. When there is a disturbance in a biopotential an action potential is resulted which is the depolarization and repolarization of the cell as illustrated in the figure below.

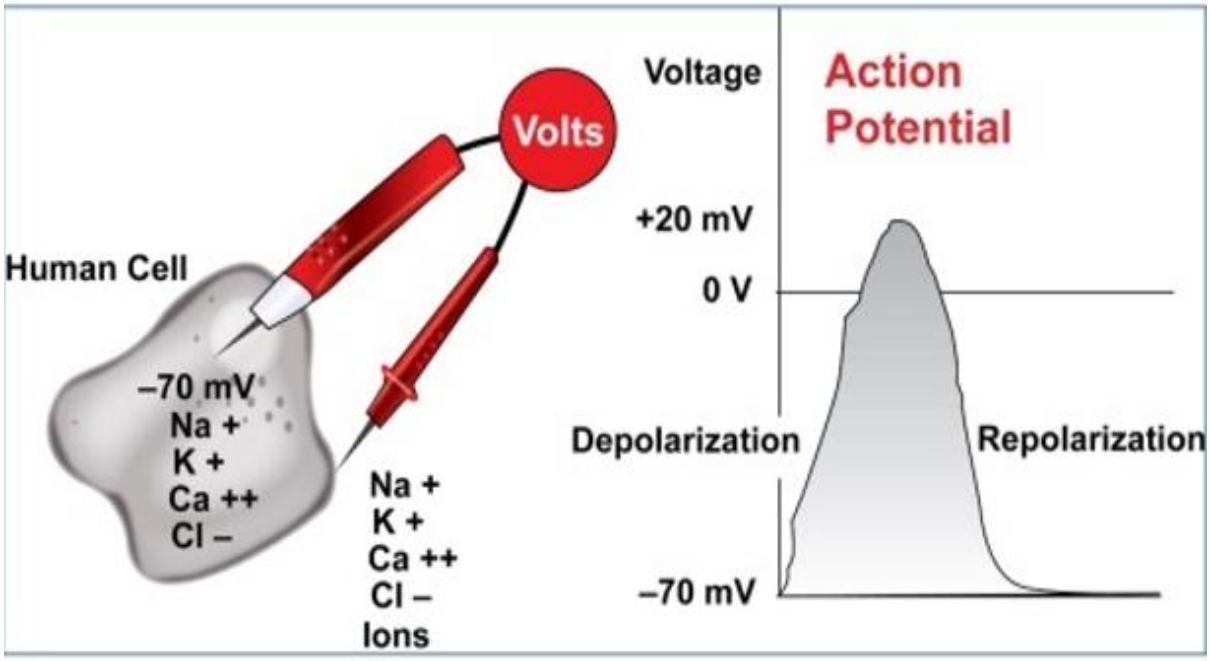

Fig. 1.1 Action potential of a cell

(Source: http://www.egr.msu.edu)

1.2 The cardiac conduction system

The heart consists of for chambers- two atria for collection of blood and two ventricles for pumping blood. The figure 1.2 shows the schematic representation of the four chambers and the major vessels connecting the heart. [1] The resting of filling phase of the cardiac chamber is called *diastole* and the contracting of the pumping phase is called *systole*.

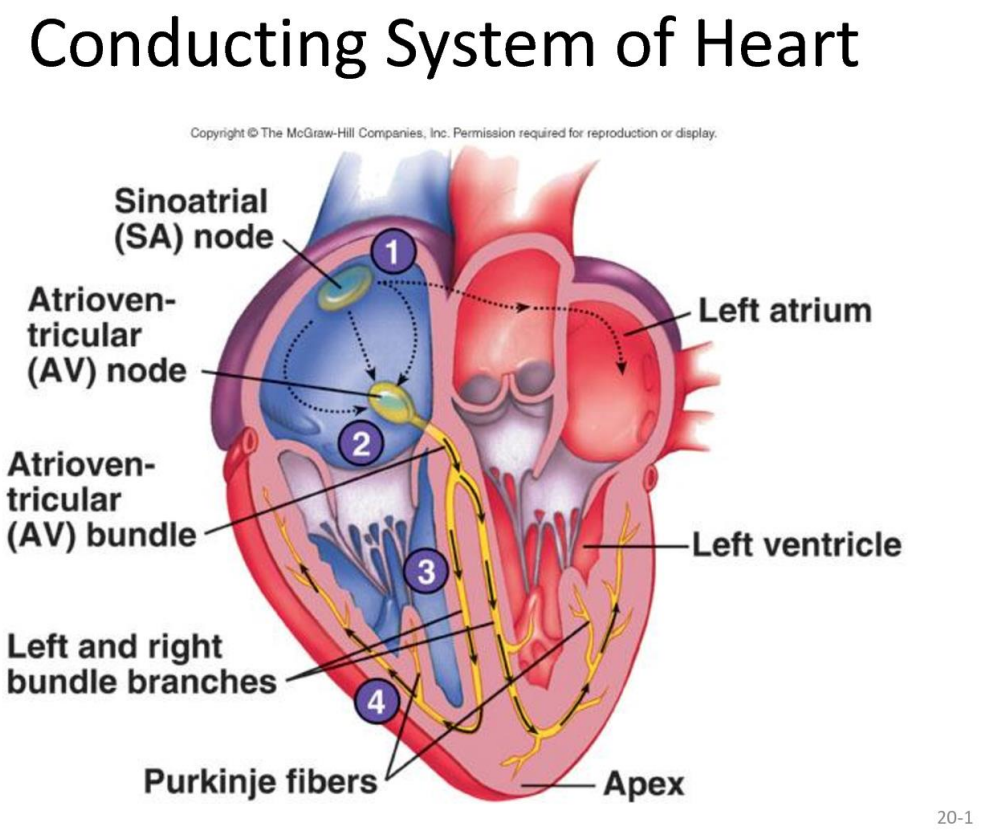

Fig. 1.2 The cardiac conduction system

(Taken from www.biologyaspoetry.com)

The right atrium (or auricle, RA) collects impure blood from the superior and inferior vena cavae. During atrial contraction, blood is passed from the right atrium to the right ventricle (RV) through the tricuspid valve. During ventricular systole, the impure blood in the right ventricle is pumped out to the lungs for Oxygenation through the pulmonary valve. The left Atrium receives purified blood from the lungs, which is passed on during atrial contraction to the left ventricle (LV) via the mitral valve. The left ventricle is the largest and most important cardiac chamber. The left ventricle contracts the strongest among the cardiac chambers, as it

has to pump out the oxygenated blood through the aortic valve and the aorta against the pressure of the rest of the vascular system of the body.

The heart rate or cardiac rhythm is controlled by specialized pacemaker cells that form the Sino-atrial (SA) node located at the junction of the superior vena cava and the right atrium. The firing rate of the SA node is controlled by impulses from the autonomous and central nervous systems leading to the delivery of the neurotransmitters acetylcholine (for vagal stimulation, causing a reduction in heart rate) or epinephrine (for sympathetic stimulation, causing an increase in the heart rate). The normal (resting) heart rate is about 70 bpm. The heart rate is lower during sleep, but abnormally low heart rates below 60 bpm during activity could indicate a disorder called *bradycardia*. In some athletes the resting heart rate is low. This condition is referred to as *training bradycardia*. The instantaneous heart rate could reach values as high as 200 bpm during vigorous exercise or athletic activity; a high resting heart rate could be due to illness, disease, or cardiac abnormalities, and is termed *tachycardia*.

1.3 The Electrocardiogram

1.3.1 The origin of ECG

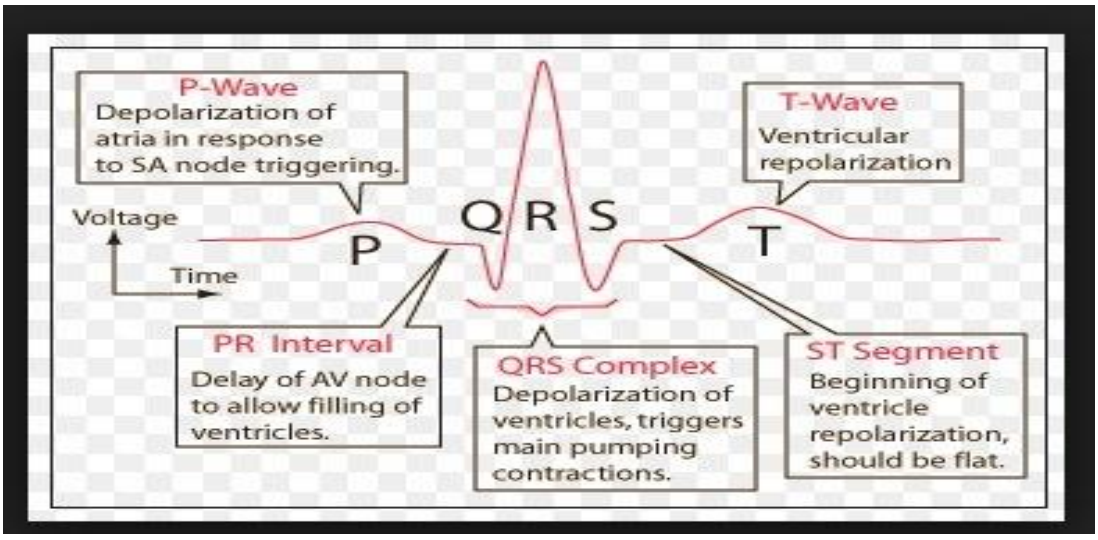

Fig. 1.3 Typical electrocardiograph

The figure 1.3 shows a typical ECG detailing the sequential process of generation of each segment in the ECG. (Taken from http://hyperphysics.phy-astr.gsu.edu)

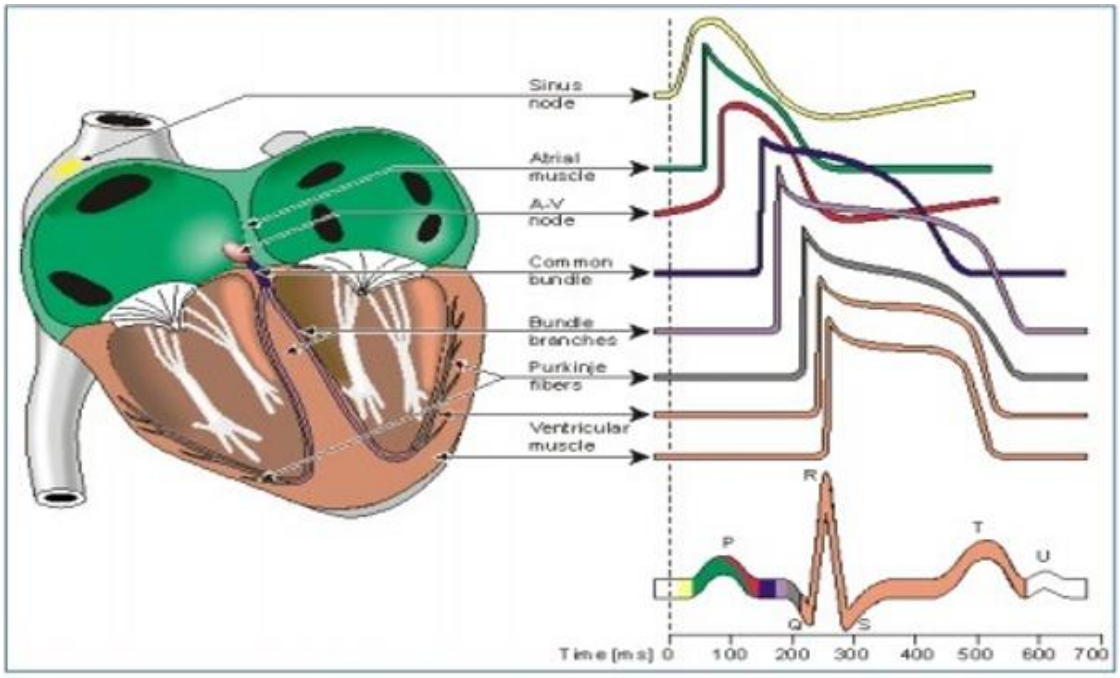

Fig. 1.4 superposition of action potentials at various nodes

(Courtesy: http://www.egr.msu.edu)

Essentially, the action potentials from different nodes are what make up Electrocardiograph signals. ECG signals are comprised of the superposition of the different action potentials from the heart beating as shown in Figure 1.4

The co-ordinated electrical events and a specialized conduction system intrinsic and unique to the heart play major roles in the rhythmic contractile activity. The SA node is the basic, natural cardiac pace maker that triggers its own train of action potentials. The sequence of events in a cardiac cycle is detailed as follows [1]:

- The SA node fires
- The Electrical activity is propagated through the atrial musculature at comparatively low rates, causing slow- moving depolarization (contraction) of the atria. This results in the P wave in the ECG. Due to the slow contraction of the atria and their small size, the P wave is slow, low-amplitude wave, with an amplitude of about 0.1 to 0.2 mV and a duration of about 60 to 80ms.
- The excitation wave faces a propagation delay at the atrio-ventricular (AV) node, which results in a normally iso-electric segment of about 60 - 80ms after the P wave in the ECG, known as the PQ segment. The pause assists in the completion of transfer of blood from the atria to the ventricles.

- The His bundle, the bundle branches and the Purkinje system of specialized conduction fibers propagate the stimulus to the ventricles at a high rate.
- The wave of stimulus spreads rapidly from the apex of the heart upwards, causing rapid depolarization (contraction) of the ventricles. This results in the QRS wave of the ECG--a sharp biphasic or triphasic wave of about 1 mV amplitude and 80ms duration.
- Ventricular muscle cell possess a relatively long action potential duration of 300 – 350ms. The plateau portion of the action potential causes a normally iso-electric segment of about 100 – 120 ms after the QRS, known as the ST segment.
- Repolarization (relaxation) of the ventricles causes the slow T wave, with an amplitude of 0.1 – 0.3 mV and duration of 120 – 160ms.
- The U wave is a small (0.5 mm) deflection immediately following the T wave, usually in the same direction as the T wave. It is best seen in leads V2 and V3. The source of the U wave is unknown. Three common theories regarding its origin are delayed repolarization of Purkinje fibres, prolonged repolarization of mid-myocardial M-cells and after-potentials resulting from mechanical forces in the ventricular wall.

1.4 Objective and scope of the project

The project deals about feasibility study of contactless ECG monitoring in the car. It envisages a method for long term cardio vascular monitoring in daily life by non-contact method of ECG recording. Two actively shielded electrodes are placed in the shoulder harness and the reference electrode is placed on the lap belt. Additionally, emphasis was laid on the use of same scheme to determine the heart rate variability of an individual using his HRV data.

As the ECG wave shape is altered by cardiovascular diseases such as myocardial ischemia and infarction, ventricular hypertrophy and conduction problems, the ECG signal obtained can be used for diagnosis purpose as in a conventional ECG. The ECG signal obtained can also be used for estimating the mental stress in an individual and also determine if the autonomous nervous system is functioning properly using the Heart Rate Variability analysis. Suitable signal processing can also be employed for different purposes like dizziness detection, sleep monitoring etc.

With regard to the above applications, a non-contact ECG measurement system can be used for continuous monitoring for the following cases:

- Driver heart rate monitoring using the seat belt setup as the project subsequently explains.
- Detecting drowsiness of the occupant.
- A person suffering from chest injury and there is no possibility of attaching electrodes to his chest.
- Heart rate and HRV monitoring in infants and premature babies and thereby facilitating early detection of SIDS.
- Persons allergic to gel.
- With a few modifications, the same scheme can be employed in the ambulance for continuous cardiovascular monitoring.

1.5 Organization of the thesis

- Chapter 1 provides information about the cardiac conduction system illustrating the sequence of events in a cardiac cycle.
- Chapter 2 gives an overview of the existing contactless ECG schemes
- Chapter 3 provides information about the heart rate variability, detailing various methods to quantify HRV.
- Chapter 4 mentions how the non-contact ECG is incorporated in the car's seat belt
- Chapter 5 deals with virtual instrumentation involved in the project and presents the experimental results
- Chapter 6 presents the conclusions and future scope.

CHAPTER 2

EXISTING NONCONTACT HR MEASUREMENT TECHNIQUES

2.1 Drawbacks of existing ECG measurement schemes

Amongst the most accurate and widely used HR determination methods are the electrocardiogram (ECG) and photoplethysmography (PPG). Although they provide reliable results when properly executed, they both are subjected to several limitations, the biggest ones being susceptibility to moving artifacts and the fact of being contact methods. As such their sensors have to be in direct and constant physical contact with the skin of the subject, making them unpleasant when used over a longer period of time or even inappropriate for specific group of patients (neonates, patients with burns, and skin diseases). Furthermore, the methods are time dependent due to drying of the conductive gel, have been known to cause allergies on the one hand (conductive gels) and can cause a certain amount of pain on the other (measuring clamp).

2.2 Noncontact ECG measurement schemes

These drawbacks of classical HR determination methods have led researches worldwide to explore the possibilities for measuring process optimization with common goal of ridding it from the mentioned limitations. As a result, several promising novel methods and measuring techniques for noncontact measurements of cardiac activity have been researched in recent years with encouraging results. The possibility of such measurements not requiring a physical contact is thought to become a valuable tool in intensive care monitoring and perhaps also on other fields (e.g., home health care, security, sports, etc.).

2.2.1 Indirect HR Measuring Based on Doppler Effect

While pumping blood through the cardiovascular system the heart undergoes volumetric changes during each cardiac cycle. These changes are then reflected on periodical movement of the subject's chest which consequently contains information about its displacement as a result of respiration activity (from 4 to 12 mm with frequencies between 0.1 and 0.3 Hz) as

well as due to beating of the heart (from 0.2 to 0.5 mm with frequencies between 1 and 2 Hz). The chest displacement can be measured by means of sensors with adequate resolution, using the principle of Doppler Effect [2].

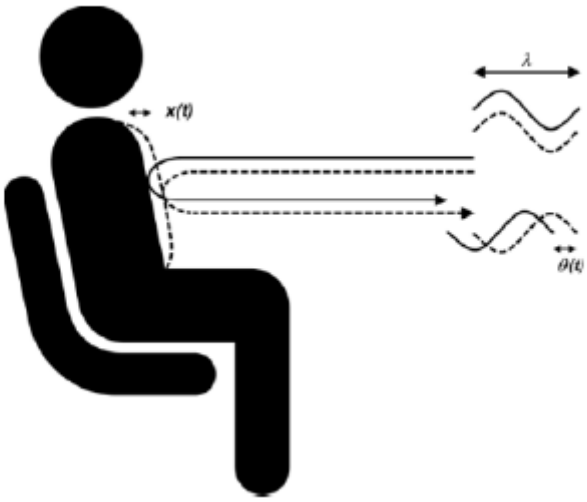

Fig.2.1 HR measurement using Doppler-effect [2].

From Fig. 2.1, if it is assumed that the receiving wave comes from a single reflection on the chest surface and the surface movements are small compared with the wavelength, then according to the Doppler Effect, the phase change $\Delta\theta(t) = 4\pi\Delta x(t)/\lambda$ where λ is the wavelength of the transmitted signal and $\Delta x(t)$ is the chest displacement [2].

2.2.1.1 Microwave Radar HR Measuring Device

The first instance of the measurement of the Doppler effect due to cardiac and respiratory activity was carried out with an off-the shelf readily available quadrature radar microwave (μW) sensor (used in automatic door application), type RSM 2650 (by B+B Thermo-Technik GmbH), shown in Fig. 2.2.a The sensor is composed of a transmitter and a receiver unit.

Fig 2.2.a [3]

(Microwave radar HR measuring device)

Fig. 2.2.b [3]

(US HR measurement)

The module has been equipped with low-noise base-band quadrature preamplifier and connected to the data acquisition (DAQ) system and as per the aforementioned relation between the phase change and chest displacement, heart rate can be calculated. The calculated power density of the used sensor at distance 30 cm from the body was S = 0.46W/m^2 (according to the "IEEE Std. C95.1, 1999 Edition" the whole body as well as partial body irradiation for uncontrolled environments must not exceed permissible level of density S = 100 W/m^2 at frequency f = 24 GHz).

2.2.1.2 US (Ultrasound) Radar HR Measuring Device:

Similar to the microwave US quadrature radar sensors can be used to detect the Doppler effect, as presented in Fig. 2.2.b Two US transducers of the same type (400PT160 by Pro-Wave Electronics Corp.) were used, operating at 40 kHz. The signal at 40 kHz and reference signals for quadrature down converter were obtained from crystal controlled oscillator operating at 10.24 MHz and divided to 80 and 40 kHz using standard HCMOS ICs. Impedance matching was done by transformers. The quadrature down-converter was built with HCMOS analogue switches (74HC4052 by Texas Instruments). Signals were amplified, low-pass filtered, and connected to the DAQ system. The measured sound pressure level (SPL) for the US radar used in the experiment was SPL = 107 dB at distance of 30 cm from the body (the International Commission on Non-Ionising Radiation Protection – ICNIRP guideline limits the exposure to airborne US to SPL = 110 dB at f = 40 kHz) [3].

2.2.2. Indirect Methods for HR Measurement Based on Audio

In every cardiac cycle two distinctive sounds are generated, the first heart sound (S1) and the second heart sound (S2), which are produced by the closing of the atrio-ventricular valves and semilunar valves, respectively. By listening to and detecting these sounds with a method known as cardiac auscultation the HR can be determined.

2.2.2a Condenser Microphone HR Measuring Device

The studio condenser microphone's polar pattern was configured to bidirectional or figure 2.3without a high-pass filter. This indicates that the microphone received the sound equally from both the front and the back of the element, while rejecting the sound received from the sides. The sound level that creates the same output voltage as the microphone does in the absence of sound (also known as the equivalent noise level) was 7 dBA SPL (datasheet NT2000).

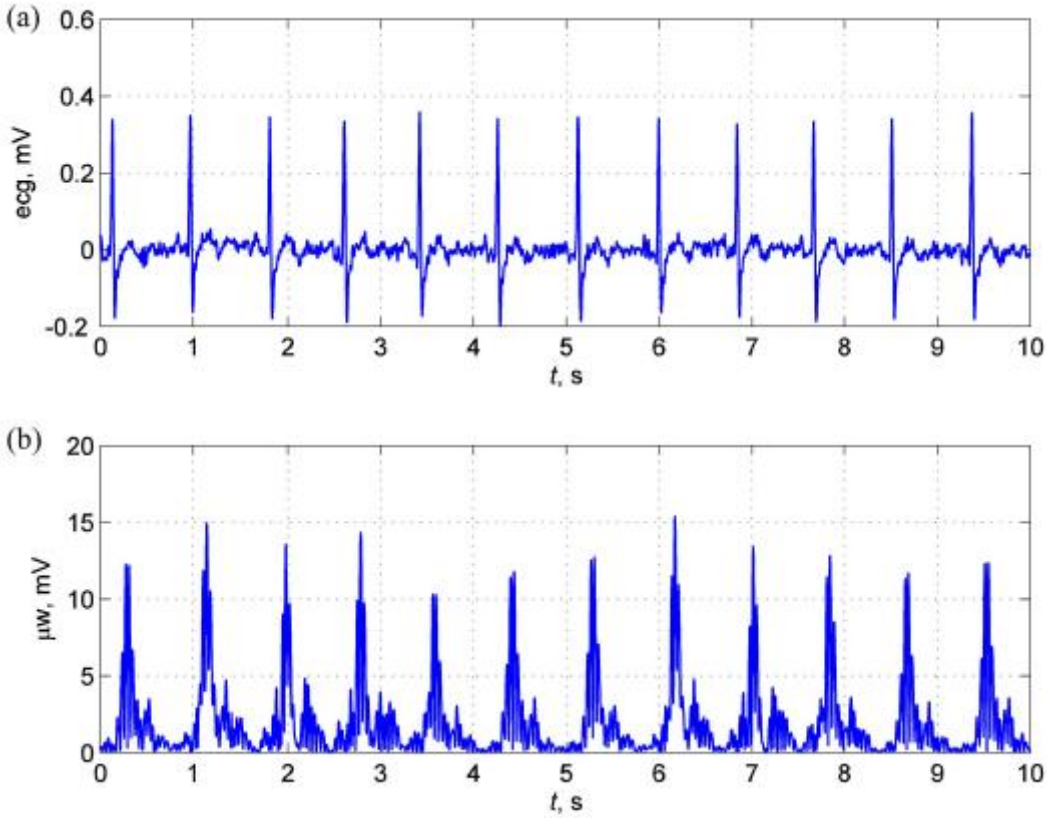

Fig. 2.3a shows a typical ECG, while 2.3b shows microwave radar sensor output after amplitude demodulation [3].

Although there is a phase lag between the two waveforms, the microwave sensor output waveform is still relevant according to the feasibility study carried out in [3].

2.2.3. Direct Methods for HR Measurement

Capacitively Coupled Electrodes:

Due to its typical amplitude (0.1–5 mV) and bandwidth (0.5–100 Hz) the ECG is relatively easy to measure compared with other biopotentials with conventional measuring methods, which rely on galvanic contact of the electronic sensor with the skin. To eliminate the need for the direct skin contact a lot of effort is being been put into finding an alternative solution.

Capacitive type electrodes (CCECG) are able to detect biopotentials with an explicit gap between the sensor and the body, even through hair and clothing and can be implemented into items of daily life. Compared with standard conductive type electrodes, the surface of these electrodes is electrically insulated and thus remains stable even in long-term applications. The sensor's metal electrode and body surface are capacitively coupled, forming a capacitance C. where

$$C = \varepsilon_r \varepsilon_o \frac{A}{d}$$

In the above equation, A is the effective surface area of the electrodes, d is the distance between the electrodes and the body, ε_r is the relative permittivity of the clothing material and ε_o is the permittivity of vacuum. As such, the capacitive type electrodes rely on detecting the so called displacement current I_D, which is proportional to the rate of change of the electric field V, associated with the ECG signal. [4]

The capacitance C depends on several factors, but usually corresponds to relatively small values from 0.1 to 10pF. For the low-frequency measurements as is the ECG, such weak coupling requires high-input impedance of the sensor as finite input resistance would attenuate V [5]. Very high impedance nodes are very susceptible to any electro-magnetic interference from the environment and motion induced artifacts which is why the electrodes need to be actively shielded to suppress the interference.

This capacitive sensing scheme has been used in many daily objects such as chair, toilet seats and beds for ubiquitous healthcare as illustrated below.

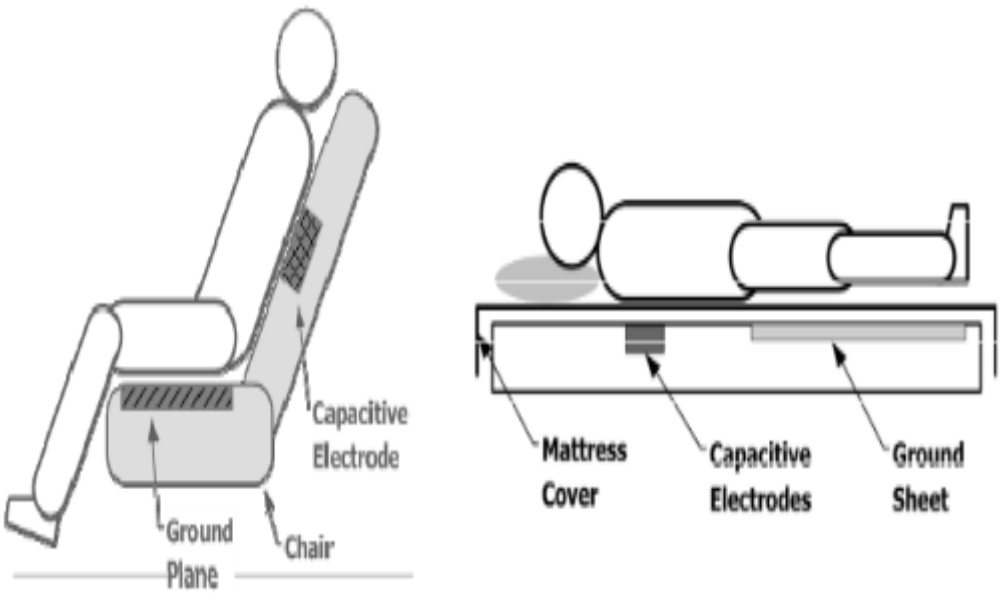

Fig.2.4 capacitive ECG in the chair (left) and bed (right) [3]

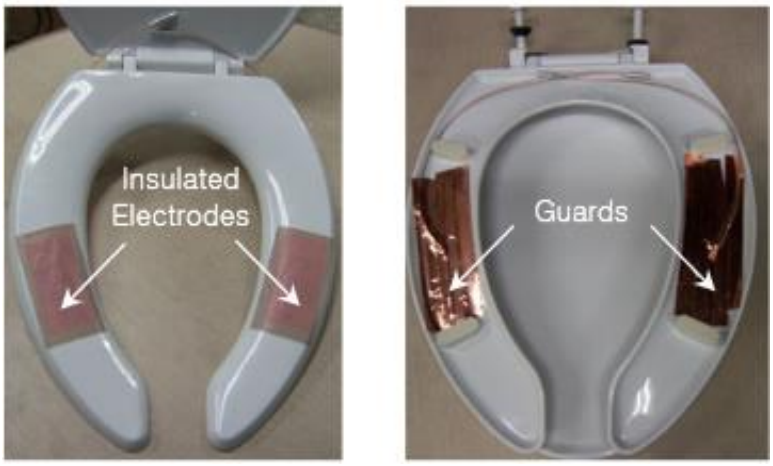

Fig. 2.5 capacitive ECG in the toilet seat [3]

Fig. 2.5 shows the insulated electrodes and shielding and Fig. 2.4 shows capacitive ECG employed for ubiquitous healthcare.

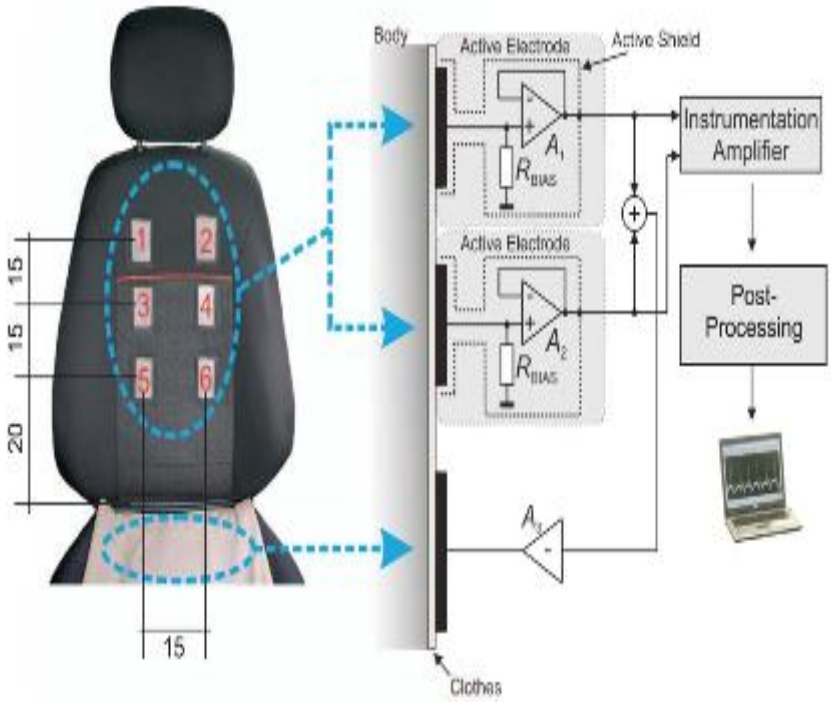

Fig. 2.6 shows schematic of noncontact ECG in the car [3]

Due to the changes in demographics and the increasing number of elderly car drivers, ubiquitous healthcare systems within the automotive environment are gaining importance. An important feature of any medical-assistance system is the reliable measurement of vital signals. One method to detect one of the most important vital signs, i.e., the ECG and secondary parameters, such as heart rate, heart-rate variability, and arrhythmias, is capacitive ECG. This is why, this scheme is being used within an automobile.

CHAPTER 3

HEART-RATE VARIABILITY

3.1 Introduction

In the last few decades, a significant relationship between the autonomic nervous system and cardio vascular mortality, including sudden cardiac death was witnessed [6]. Experimental evidence for an association between an inclination for lethal arrhythmias and signs of either increased sympathetic or reduced vagal activity has driven the development of quantitative markers of autonomic activity.

Heart rate variability (HRV) represents one such markers which is also one of the most promising. The apparently easy derivation of this measure has led to its popularity in the clinical circles. 'Heart rate variability' has become the conventionally accepted term to describe variations of both the instantaneous heart rate and RR intervals. In order to describe the oscillations in consecutive cardiac cycles, other terms have been used in the literature, for instance, cycle length variability, RR variability and RR interval tachogram and they appropriately emphasize the fact that it is the interval between the consecutive beats that is being analysed rather than the heart rate per se. A higher HRV is desirable as a lower HRV indicates acute emotional strain stress anxiety and a greater frequency and duration of daily worry [7].

3.1.1 Background

The clinical relevance of HRV was first appreciated in as early as 1965 when Hon and Lee [8] observed that foetal distress was the immediate consequence of alterations in beat to beat intervals rather than the changes in the heart rate itself. During the 1970s, researchers devised simple bedside tests of short-term RR differences to detect autonomic neuropathy in diabetic patients. The association of post-infarction mortality and reduced HRV was first established by Wolf et al, in 1977 [8]. Power spectral analysis of heart rate fluctuations to quantitatively evaluate beat-to-beat cardiovascular control was introduced by Akselrod et al in 1981 [8]. The

clinical relevance of HRV became apparent in the latter half of 1980s when it was confirmed that HRV was a strong and independent predictor of mortality following an acute myocardial infarction. With the advent of new, digital, high frequency, 24-h multi-channel ECG recorders, HRV has the potential to provide valuable insights into physiological and pathological besides providing better risk assessment.

3.2 Quantifying HRV

Variations in the heart rate can be measured using the following tools [8]:

- Tools that measure the statistical properties of the data (often referred to as geometrical indices as they attempt to categorise the shape of a histogram of RR intervals).
- Tools that evaluate statistics in the time domain.
- Metrics that facilitate the frequency domain analysis of the RR tachogram.
- Non-linear methods using the Poincaré plot.

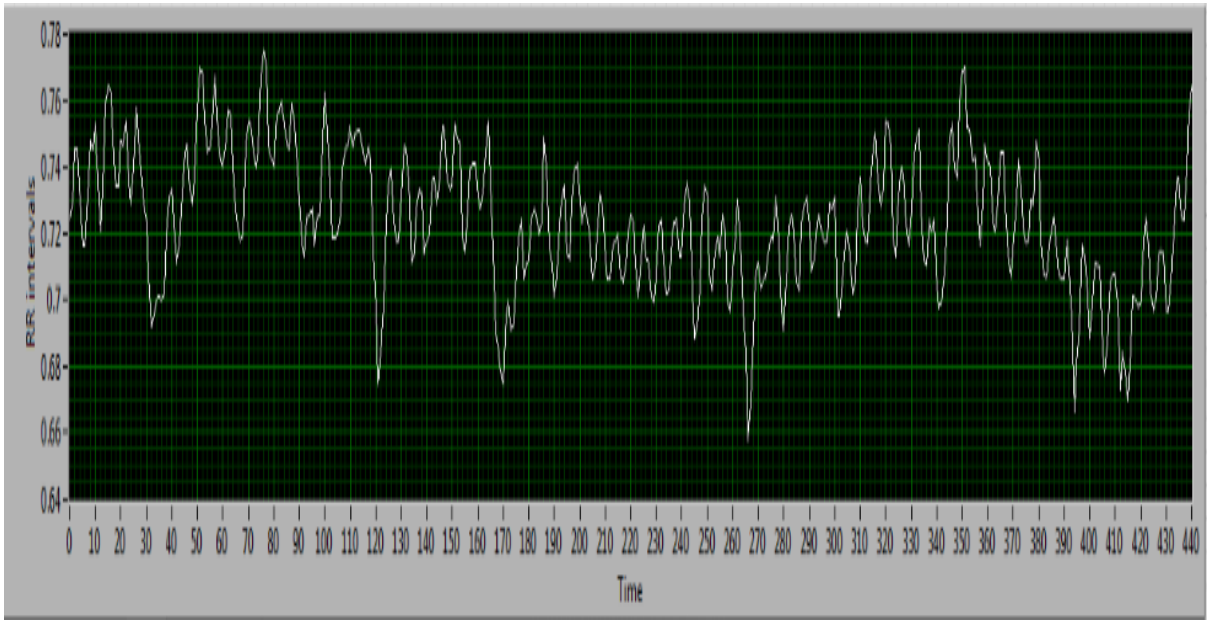

Fig 3.1 A typical RR tachogram

(Taken from analyses in the ‘RESULTS’ section of this thesis)

3.2.1 Geometric methods:

HRV indices that are generally referred to as geometric methods, attempt to quantify the shape of the histogram of the RR tachogram. A basic measurement of the geometric pattern (e.g. the width of the distribution histogram at the specified level) is converted into the measure of HRV. The geometric pattern is interpolated by a mathematically defined shape (a triangle for instance). A typical histogram is shown below

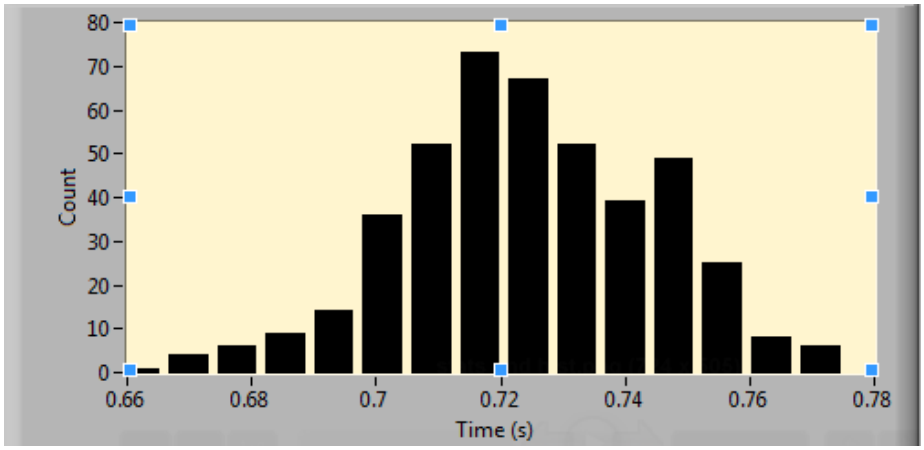

Fig. 3.2 A typical RR interval histogram

(Taken from analyses in the 'RESULTS' section of this thesis)

The count on the Y-axis is the number of RR interval pairs in the RR tachogram against their respective intervals (plotted on the x-axis) that were used to plot the histogram shown above. The x-axis shows the time interval between each RR pair. There are two tools by means of which the connection between the geometric shape fitting and HRV can be understood: The *HRV triangular index* is the total number of all NN intervals (count) divided by the maximum of the density distribution. The other tool is the *TINN- Triangle interpolation of NN interval histogram*. It is the base of the triangle, measured in ms (from the histogram).

One vital motivation for developing histogram based HRV methods is their relative robustness to inclusion of non-NN intervals (or the normal RR intervals) caused by ectopic beats or artefacts. Such intervals usually tend to fall outside the dominant peak of the RR interval histogram [8]. One limitation of using histogram-based HRV is that the data acquisition period should not be less than 24-hours. Since a 24-hour recording contains periods from day activities as well as from rest during the night. As a result, the use of triangular methods is not advisable as they tend to overestimate the variability in the heart rate [8]

3.2.2 Statistical indices

Statistical HRV indices are calculated on a beat-to-beat basis and are based on Euclidean root-mean square (rms) metrics. The time series indices are broken down to the following categories [9].

- Variables directly derived from the beat-to-beat intervals, such as the mean HR and the standard deviation (SD) for the entire recording period.
- Variables based on the differences between adjacent cycles (or RR pairs), such as the proportion of difference between adjacent cycles that exceed an arbitrary limit.

The Task Force of the European Society of Cardiology and the North American Society of Pacing Electrophysiology (NASPE) recommend the following indices:

SDNN (ms): Standard deviation of all NN intervals (also known as SDRR) usually over 24 hours.

SDANN (ms): Standard deviation of the averages of NN intervals in all 5-minute segments of the entire (24-hour) recording.

RMSSD (ms): The square root of the mean of the sum of the squares of differences between adjacent NN intervals.

SDNN index (ms): Mean of the standard deviations of all NN intervals for all 5-minute segments of the entire (24-hour) recording.

SDSD (ms): Standard deviation of differences between adjacent NN intervals.

NN50 (count): Number of pairs of adjacent NN intervals differing by more than 50 ms in the entire recording;

pNN50 (%): Percentage of adjacent NN differing by more than 50ms over an entire 24-hour ECG recording.

Heart rate variability reduces with age as demonstrated by [10] but is usually higher in athletes as established by Ande E. Aubert et al. Hence, HRV can sometimes be used to detect OT-Overtraining syndrome in the athletes to assess their autonomic activity [11].

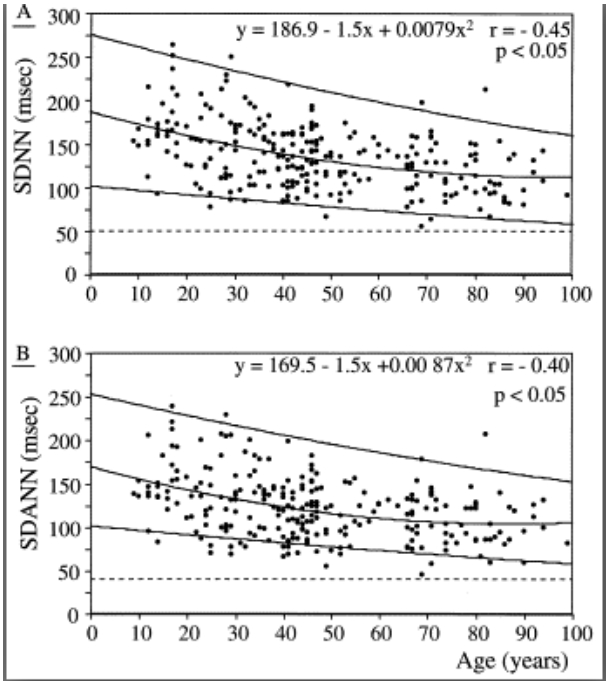

Fig 3.3 HRV metrics on Y- axis and Age on X-axis [10]

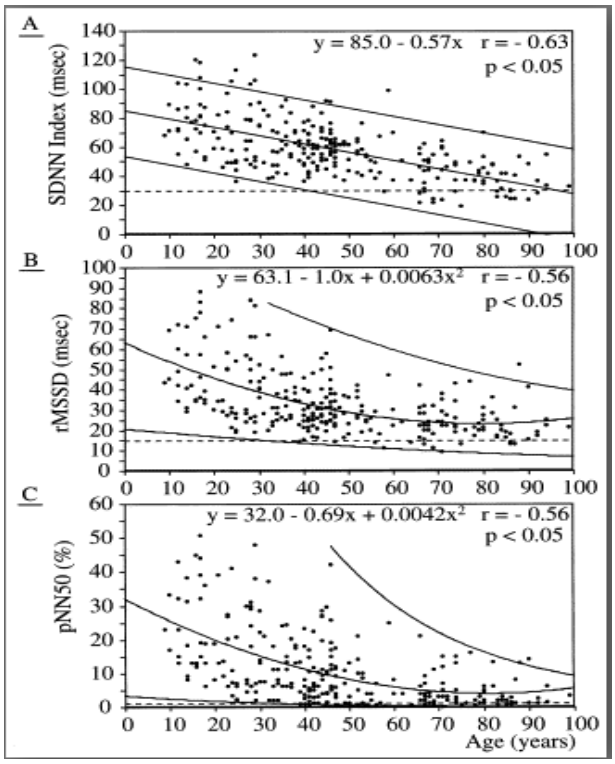

Fig 3.4 Age on X-axis and the HRV parameters on the Y-axis [10]

3.2.3 Frequency domain methods

Heart rate changes occur on a wide range of time scales; millisecond sympathetic changes stimulated by exercise cause an immediate increase in HR resulting in a lower long term

baseline HR and increased HRV over a period of weeks and months. Similarly, a sudden increase in blood pressure will lead to a sudden semi-permanent increase in HR. Similarly respiration also affects the HR- inspiration causes increase in the heart rate whereas expiration causes a decrease in the heart rate. In order to better understand the contributing factors to HRV and the time scales over which they affect the heart, it is useful to consider the RR time series (or tachogram) in the frequency domain.

3.2.3.1 Power Spectral Analysis

Power spectral analysis was first introduced into HRV analysis in 1981 by Akselrod et al[8]. The frequency spectrum of an RR interval tachogram has been split into four frequency bands:

- ULF: Ultra-low frequency: 0.0001Hz to 0.003Hz
- VLF: Very-low frequency: 0.003Hz to .04Hz
- LF: low-frequency: 0.04Hz to 0.15Hz
- HF: High-Frequency: 0.15Hz to 0.4Hz

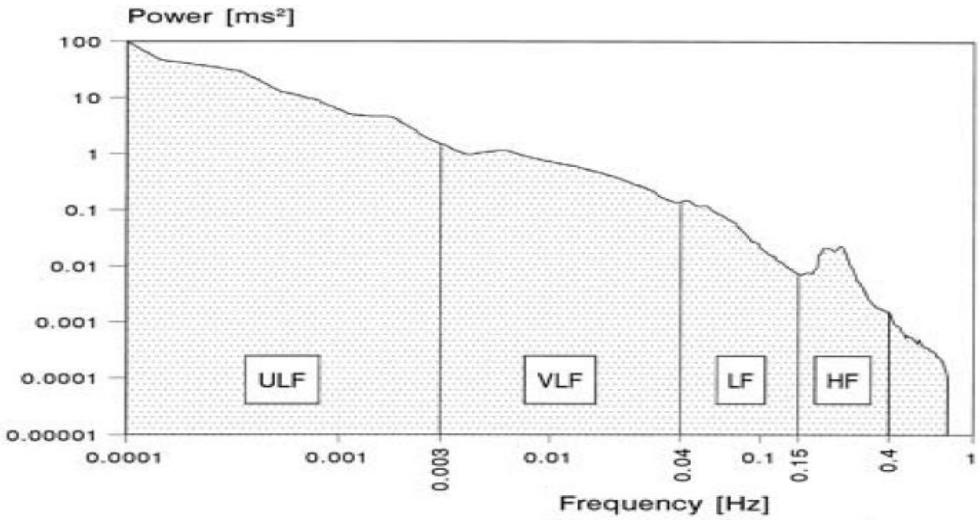

Fig 3.5 typical FFT of the RR interval tachogram (time series) for a 24-hour period [8]

Demarcations are made to split the different frequency ranges with the power being represented in millisecond-squared because, the power (or variance) is the square of the standard deviation (expressed in ms). The motivation for splitting the spectrum into these frequency bands lies in the belief that the distinct biological regulatory mechanisms that contribute to HRV act at

frequencies that are confined (approximately) within these bands. Fluctuations below 0.04Hz in the VLF and ULF bands are thought to be due to long-term regulatory mechanisms such as the thermoregulatory system, the reninangiotensin system (related to blood pressure and other chemical regulatory factors) and other humoral factors [16]. It is generally accepted in the clinical community that the HF band is the measure of the parasympathetic outflow [16]. However, the physiological interpretation of the LF band is subject to controversy and although both sympathetic and parasympathetic mechanisms can have a bearing at these frequencies, fluctuations in the LF band are widely attributed to the sympathetic activity only [16]. It is also worthwhile to note that the region below 0.4Hz is the region of interest since the respiratory modulation frequency is the highest component of a HRV signal (RR tachogram) and this is rarely above 20 rpm (about 0.33Hz).

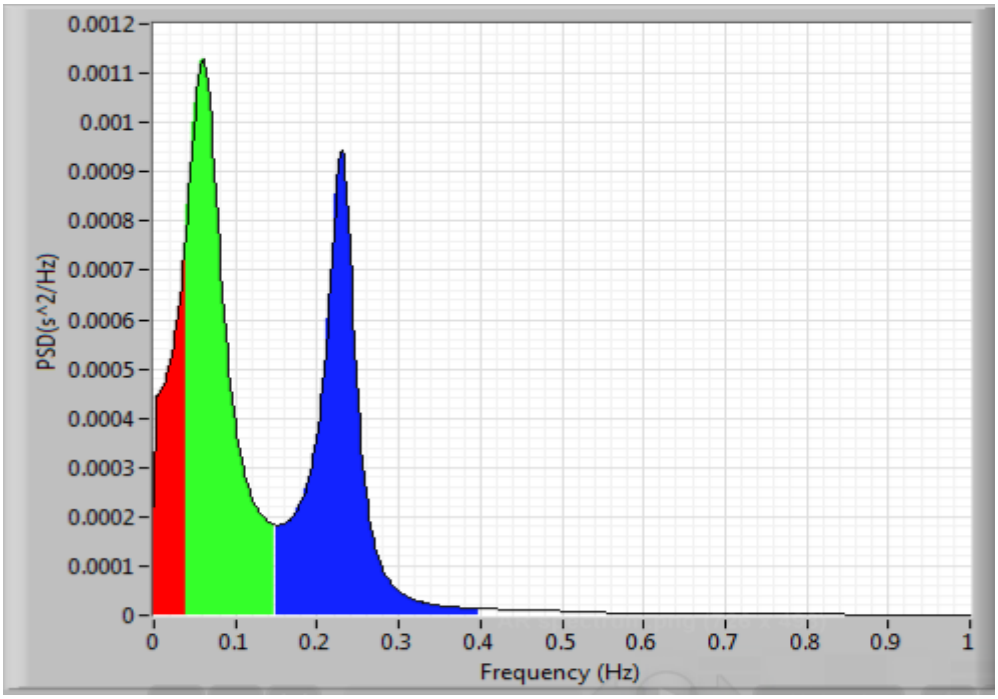

Fig 3.6 shows a typical PSD graph using the AR method

(Taken from analyses in the 'RESULTS' section of this thesis)

Figure 3.7, shows the power spectral density of the RR tachogram of a 35 year old subject. The two dominant are peaks shown. The lower peak indicates the *Mayer waves.* This is where the

BP fluctuations occur according to [12]. The higher frequency peak (around 0.25Hz) signifies the respiratory effects on the heart rate variability.

3.2.3.1.1 LF/HF ratio and the sympathovagal balance

Rhythms within the HF band, synchronous with the respiration rate, are due to the intra-thoracic pressure changes and mechanical variations caused by the action of breathing. The manifestation of the respiration rhythms on the RR tachogram is known as Respiratory Sinus Arrhythmia (RSA) as can clearly be seen in figure 3.5. This higher frequency peak (above 0.15 Hz) is mediated almost exclusively by fluctuations of the vagal-cardiac nerve activity [13] and is generally accepted as a marker of parasympathetic activity [14]. The 0.1 Hz peak corresponding to the most dominant of the Mayer waves is mostly mediated by fluctuations of sympathetic nerve activity [15]. Although sympathetic and parasympathetic mechanisms are involved in the LF band, an increase in LF power has always been observed as a consequence of sympathetic activation such as rest-tilt maneuvers, mental stress, haemorrhage, and coronary occlusion [15] (refer to figure 3.7). An increase in LF power is therefore widely accepted as a marker of sympathetic activation. Since physiological interventions produce reciprocal changes of sympathetic and vagal outflows, it has been suggested [16] that the balance between these opposing neural regulatory mechanisms can be quantified by the ratio of the power in the LF to the power in the HF band (LF/HF) which is then taken as a measure of the sympathovagal balance. Although this metric is generally thought to quantify the relative contributions of the two branches of the CNS, this idea remains a topic of much debate amongst clinicians. Nevertheless, there is a consensus that this is a useful model for clinical applications [15].

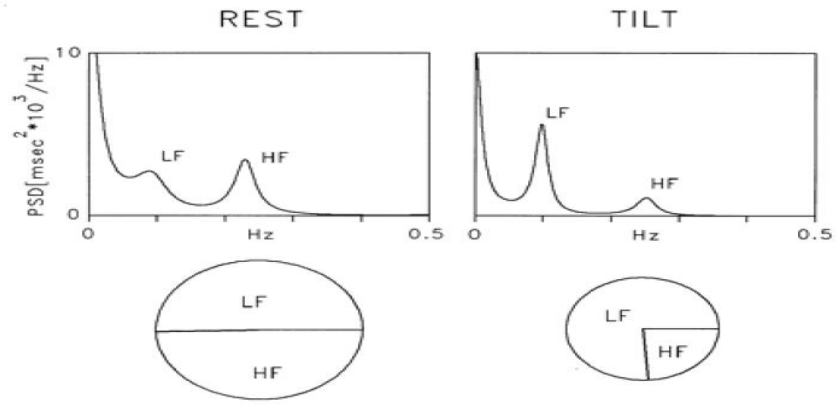

Fig 3.7 shows LF/HF during rest and tilt [8]

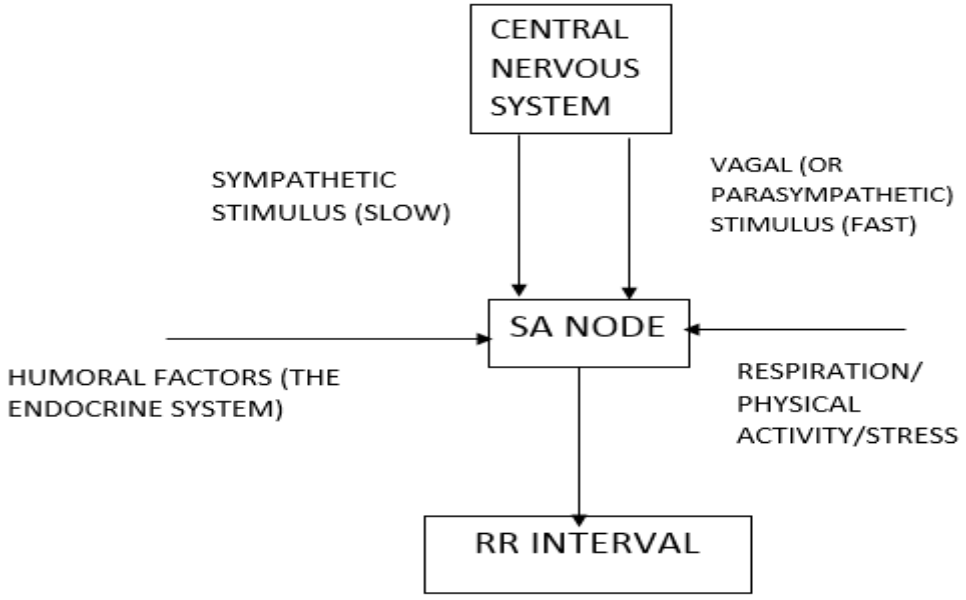

Fig 3.8 shows various parameters affecting the RR interval tachogram

3.2.4 Non-linear methods

The heart rate variability is a non-linear phenomenon. It has been speculated that analysis of HRV based on the methods of non-linear dynamics might elicit valuable information for the physiological interpretation of HRV and for the assessment of the risk of sudden death. The Poincaré plot is the most commonly used tool to quantify the non-linear dynamics of HRV. It is basically a visual representation of the RR intervals from an RR tachogram (time-series) into a simplified phase space or the Cartesian space. A series of these points at successive times outlines a curve (an ellipse), or trajectory, that describes the system's evolution and therefore is commonly applied to assess the dynamics of heart rate variability.

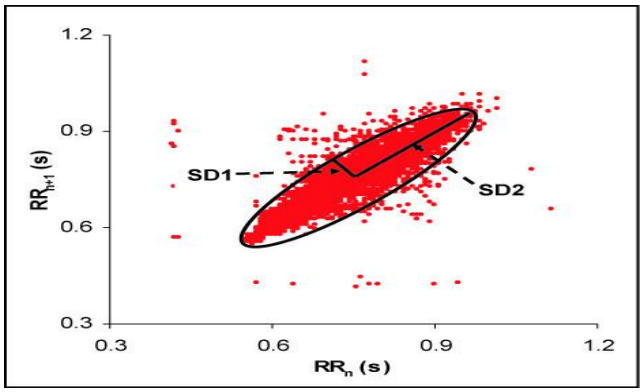

Fig 3.9 a typical Poincaré plot [18]

The figure shows a standard Poincaré plot drawn with the next RR interval (seconds) on the Y-axis and the respective preceding RR intervals on the X-axis. Analysis of the Poincaré plot gives us two important parameters such as Standard Deviation1 (SD1) and Standard Deviation2 (SD2) after the elliptical shape has been outlined after plotting the graph. SD1is the length of the minor axis whereas SD2 is the length of the major axis. Physiologically, the SD1 is a measure of rapid changes in R–R intervals and because vagal effects on the sinus node are known to develop faster than sympathetically mediated effects, it is considered a parasympathetic (vagal) index of sinus node control [17] and SD2 indicates both the sympathetic and parasympathetic influences on the SA node [18].

CHAPTER 4

NON-CONTACT ECG INTEGRATED INTO THE SEATBELT OF A CAR

4.1 Introduction

Seat belts were invented by English engineer George Cayley in the early 19th century, though Edward J. Claghorn of New York, was granted the first patent. A seat belt, also known as a safety belt, is a device designed to secure the occupant of a vehicle against any harmful movement that may result due to a collision or a sudden stop. A seat belt functions to reduce the likelihood of death or life threatening injury in the event of an accident by reducing the force of secondary impact with the risk of interior strike hazards, by keeping the occupants positioned correctly for maximum effectiveness of the airbag (if equipped) and by ensuring the occupants are not ejected from the vehicle during a crash or a vehicle-rollover. The seat belt is pressed against the occupant at all times thereby applying an opposite force on him to prevent him from falling out of the vehicle.

There are different types of seat belts viz., two point, three point and so on depending on the number of end points it is attached at. The three point Belt in Seat (BIS) is the most commonly used configuration in modern day automobiles. It consists of a 'Sash belt' (also known as a shoulder harness) and a 'lap belt'. The belt is attached at three endpoints within the automobile.

Fig 4.1 A typical 3-point BIS configuration

(Source: http://www.gov.bm/portal/erver.pt/portal)

4.1.1. Motivation

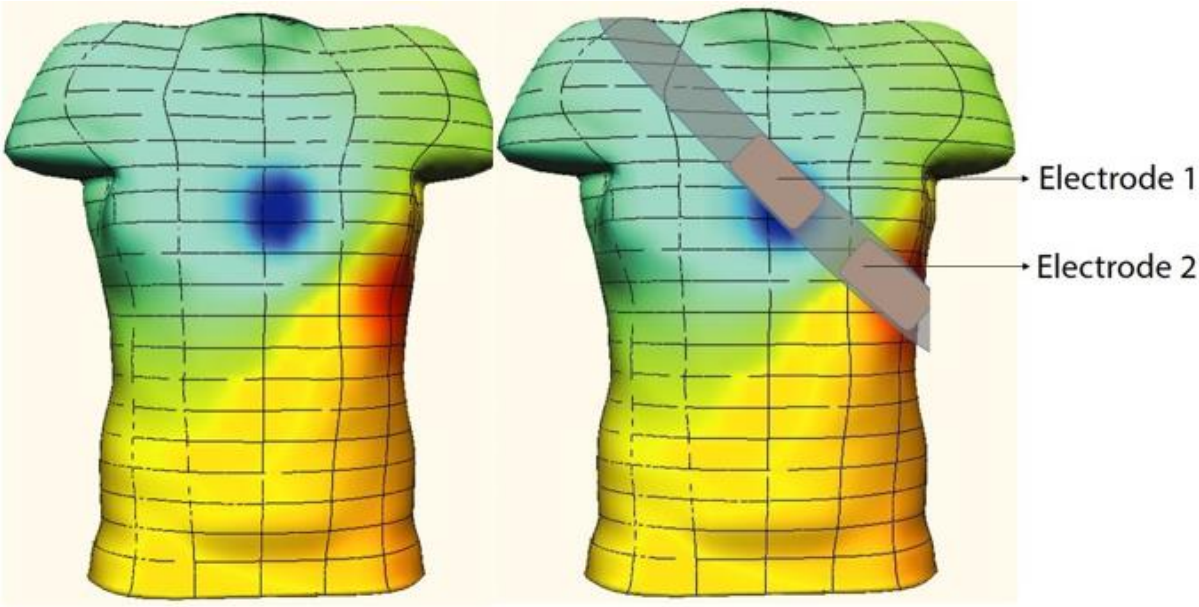

Figure 4.2. Electric field distribution along the human torso and the corresponding electrodes

(Image courtesy: www.naturereviews.com)

The figure above depicts the anatomical model of the upper part of the human body. It represents varying electrical conducting properties of the tissues, such as skin, bone, or the musculature. The heart generates electric fields in the torso. These electric fields are modelled in colour in the above diagram. ‘Red’ represents positive potentials, while the ‘blue’ represents negative potentials. By suitably placing the electrodes in the areas on the torso where the electric field concentration is the highest, the bio-potentials can be recorded. The figure on the right shows that the electrodes are placed in the areas shown in the figure for maximum capacitive coupling. This placement of electrodes not only made the capacitive coupling maximum but also rendered the signal acquisition better. This illustration, along with the fact that the seat belt is continuously pressed against the occupant, was the impetus behind the idea of placing the electrodes on the seat belt of a car for ubiquitous heart-rate and, consequently, the heart rate variability monitoring over a finite period of time, most importantly, without any direct electrode contact with the skin. The signal acquisition could be possible due to the capacitive coupling between the electrode and the skin-interface (in this case the clothing).

(Image courtesy: www.naturereviews.com)

4.2 Electrode configurations

4.2.1 Electrode configuration 1

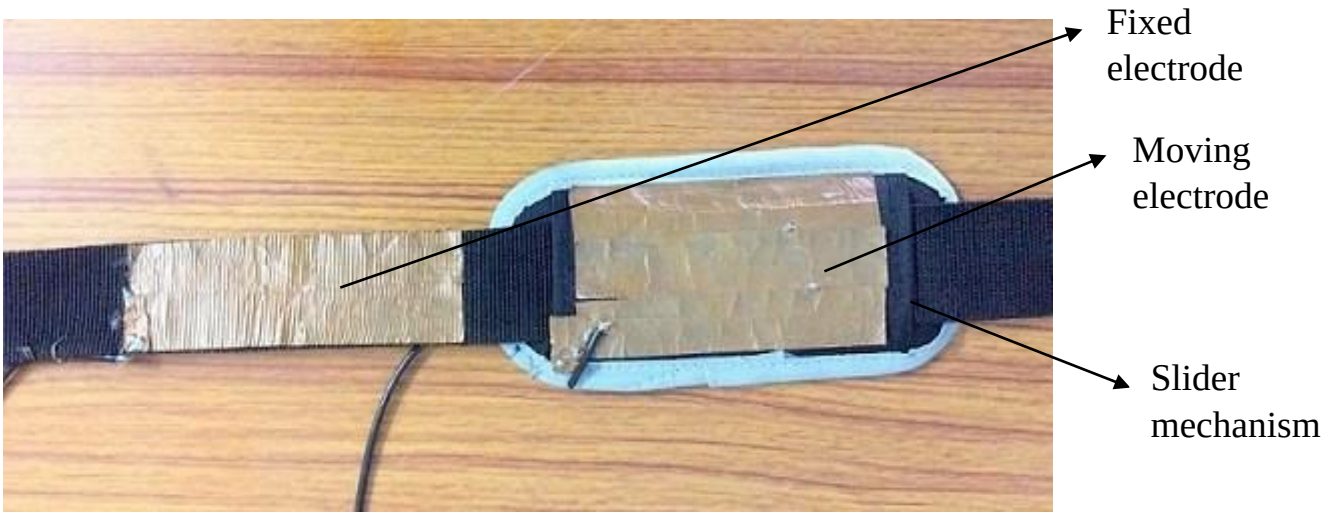

Figure 4.3. A prototype of Seat-belt with electrodes.

In order to verify the quality of the ECG recording, a seat belt prototype (depicted in the figure above) with the electrodes was developed from a belt salvaged from a handbag. This prototype was designed in such a way that one of the electrodes was placed on a slider mechanism while the other electrode was immovable. The reference electrode was positioned on the seat underneath right thigh. The function of the sliding electrode was to determine at what position, the ECG could be recorded satisfactorily. As demonstrated in the subsequent figures, the coupling was the most effective when the slider was placed at the exact centre of the chest (roughly near the celiac plexus). Any slight deviation in the position either to the left or right of the centre rendered the capacitive coupling relatively less strong thereby impacting the quality of the ECG recording.

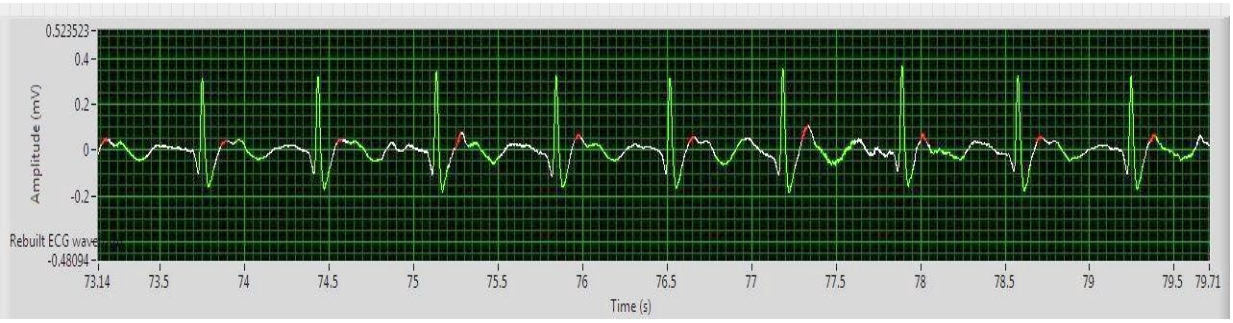

Fig. 4.4 ECG when the slider was positioned at the centre of the chest

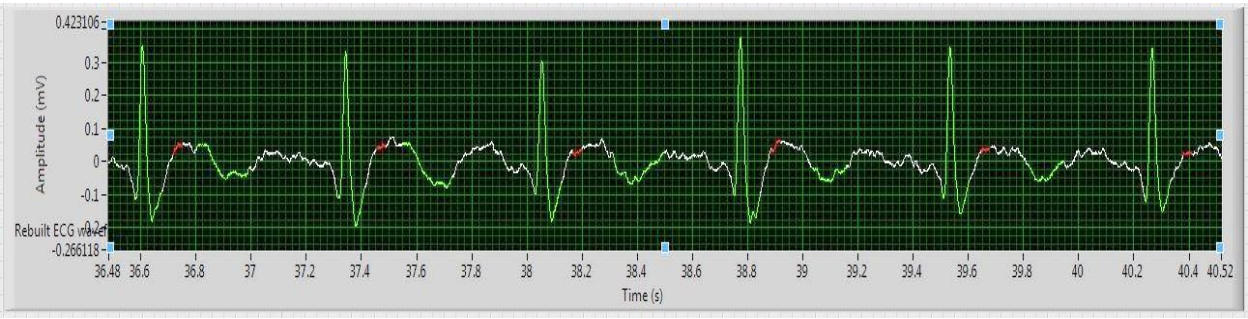

Fig. 4.5 ECG when the slider was positioned slightly to the left of the chest's centre

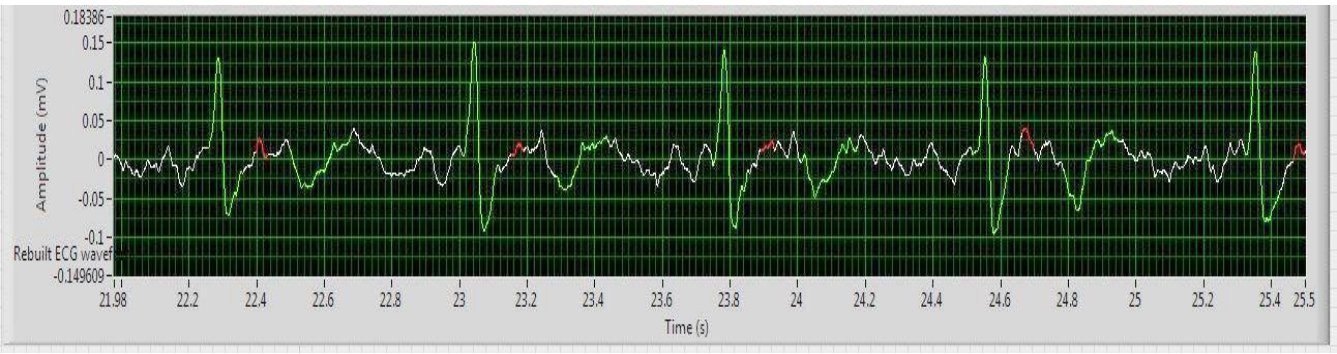

Fig.4.6 ECG when the slider was moved slightly to the right

The above observations reinforce the premise that the electric field that is influenced by the heart is the highest along the region depicted in the figure 4.2. Also, the capacitive coupling is the strongest along that region. This observation helped our analysis regarding the appropriate placement of the capacitive sensors on the seat belt and consequently facilitating better ECG recording.

4.2.2. Electrode configuration-2:

After the optimal placement of electrodes was determined, they were incorporated on an actual seat belt. Subsequently, shielding for the electrodes was also incorporated on to the same seat belt and the seat belt itself was fitted on a seat. The electrodes were made from the same conductive tape that was used in the previous configuration.

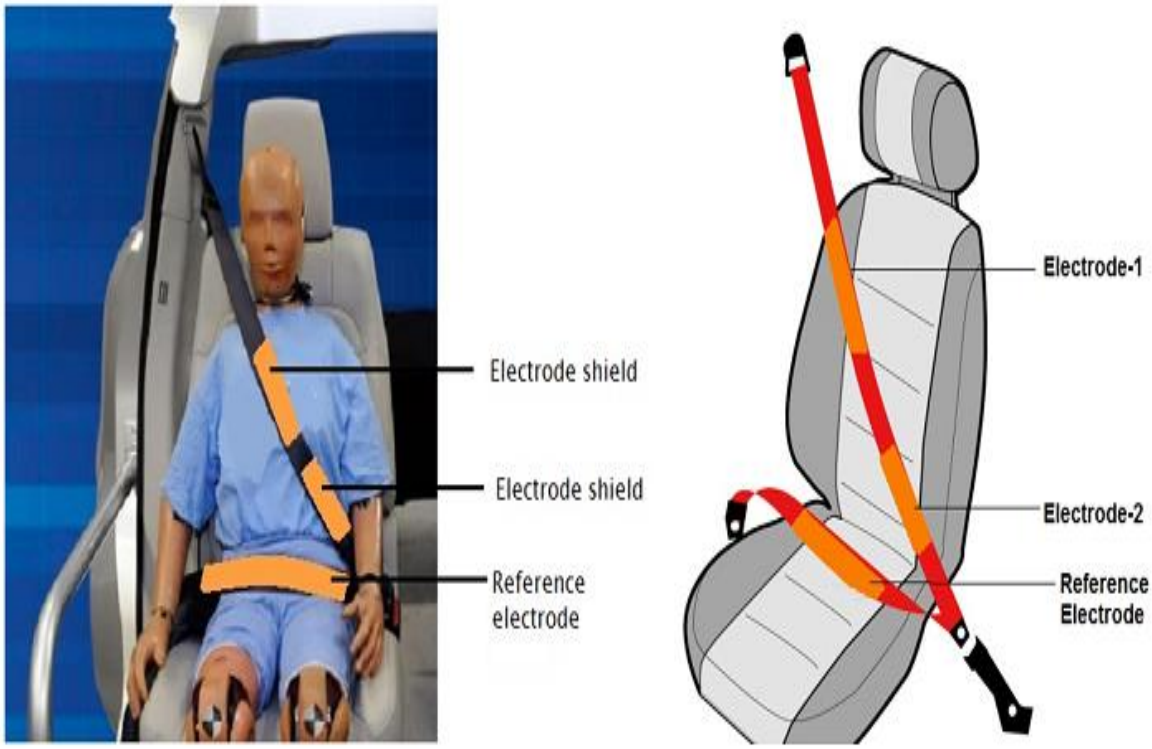

Fig. 4.7 shows the electrodes (Right) and their respective shields (left)

(Images sourced from www.google.com)

As depicted in the figure 4.7, the two-electrodes to be connected to the differential amplifier were placed on the sash belt (or the shoulder harness) and the reference electrode was placed on the lap belt. The figure on the left shows the electrode shields of the two electrodes whereas the electrodes themselves were placed just below the shields on the inner surface of the sash belt; these electrodes are in contact with the occupant's clothing. The figure on the right depicts the inner surface of the shoulder harness on which the electrodes were placed. The reference electrode has no shielding. Hence, the inner surface of the lap belt shown in both the diagrams depicts the reference electrode only and not the shield.

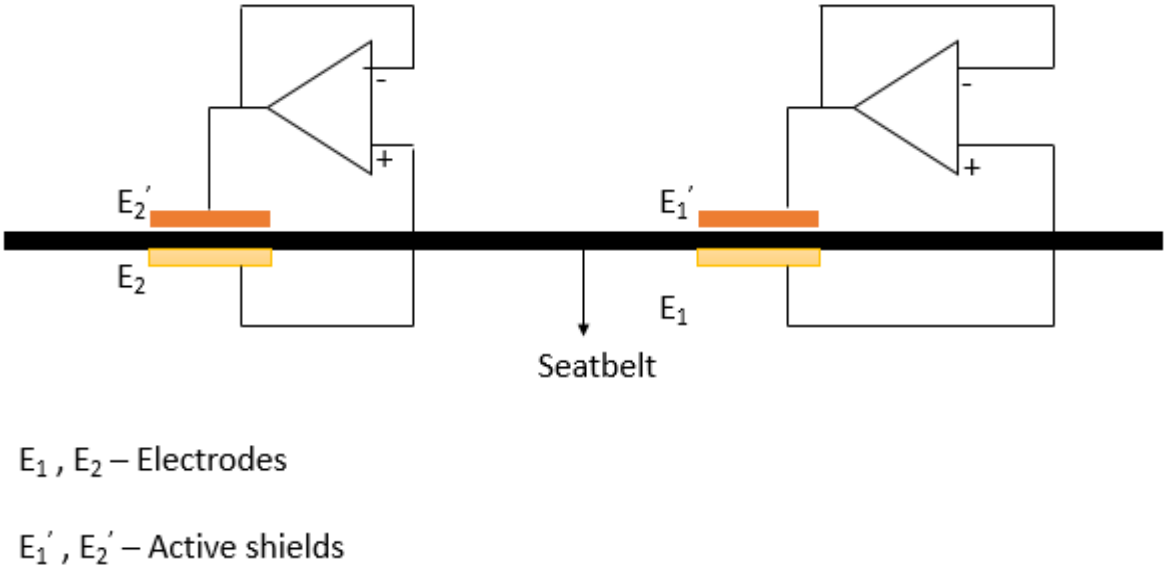

Fig. 4.8 Electrodes and shields along with the seatbelt

Fig 4.9 shows a subject wearing a single layered shirt (T-shirt) whose ECG is being recorded

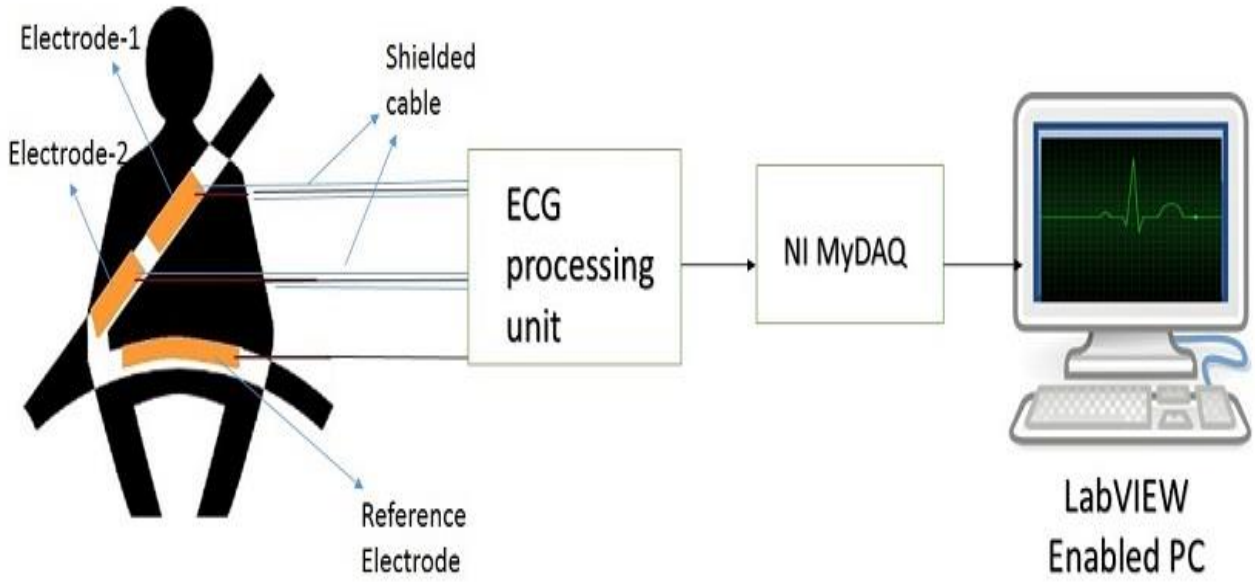

Fig 4.10 Block diagram highlighting the entire acquisition procedure

Fig 4.9 shows the block diagram of the ECG acquisition from the electrodes placed in the seat belt. The dashboard seat belt logo is shown along with the three electrodes in their respective positions. Signal acquisition takes place via shielded cables. The filtered ECG from the 'ECG processing unit' is then acquired for post-processing on a PC using LabVIEW environment wherein the mean heart rate and consequently the Heart Rate Variability (HRV) metrics are calculated and the HRV trends are plotted on a graph.

CHAPTER 5

VIRTUAL INSTRUMENTATION AND EXPERIMENTAL RESULTS

5.1 Acquisition

The ECG waveform was acquired using NI myDAQ, with a sampling rate of 1000Hz, with the total number of samples acquired being constant at 5000.

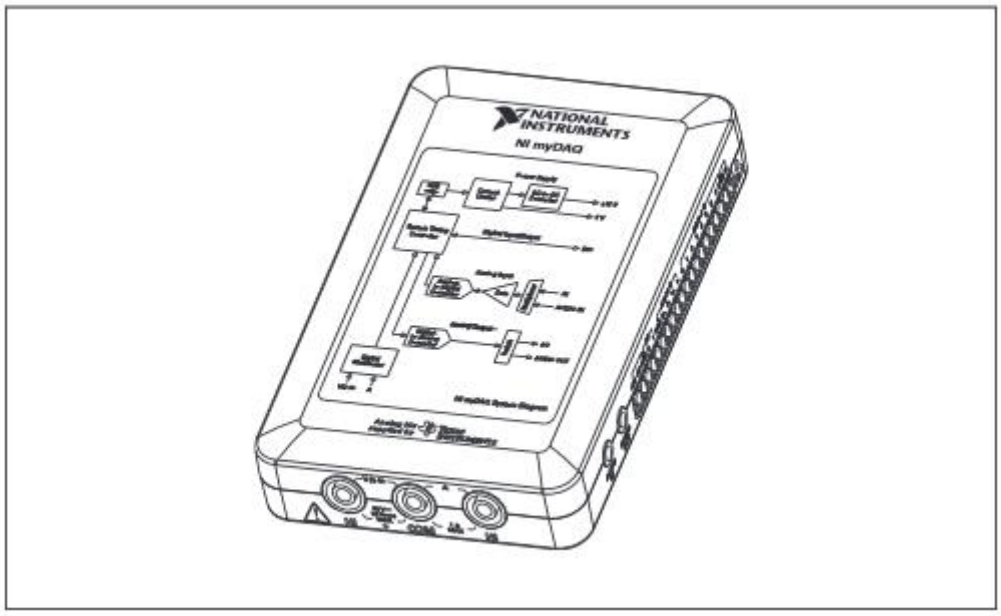

Fig 5.1 NI myDAQ (taken from www.ni.com)

NI myDAQ is a low-cost portable data acquisition (DAQ) device that uses NI LabVIEW based software instruments, allowing users to measure and analyze real-world signals like the ECG. It has two analog input channels and two analog output channels. So the input can be acquired as a maximum sampling rate of 200 kS/s or the output waveform can be updated at 200 kS/s. Additionally, there are 8 Digital IO lines on myDAQ device. +15V, -15V and the analog ground also feature on this device so there is no need of external power source once it is plugged to a computer via USB.

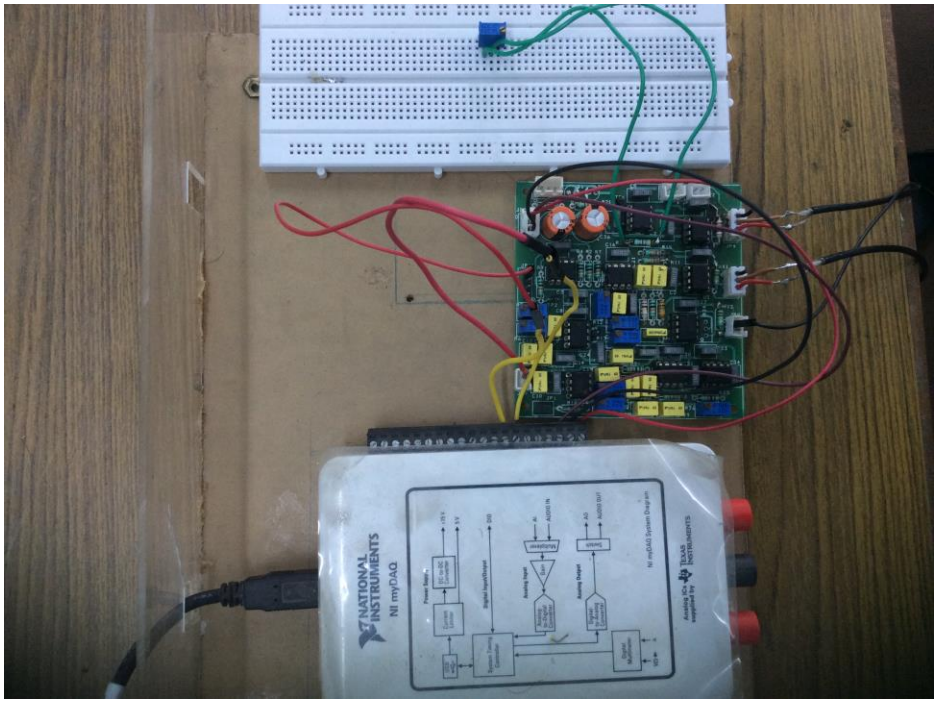

Fig. 5.2 Signal processing and signal acquisition unit [21]

Figure shows the signal processing unit placed beside a data acquisition device. The signal processing unit consists is highly robust. It consists of an instrumentation amplifier, a 0.4Hz-35Hz band-pass filter, and a notch filter to remove 50Hz power line interference. The band-pass filter is realized by cascading a 0.4Hz high-pass filter and a 35Hz low-pass filter. The high-pass filtering action is achieved by subtracting the low-pass signal from the instrumentation amplifier output by the relationship 1-LPF=HPF due to the high frequency noise introduced by the HPF.

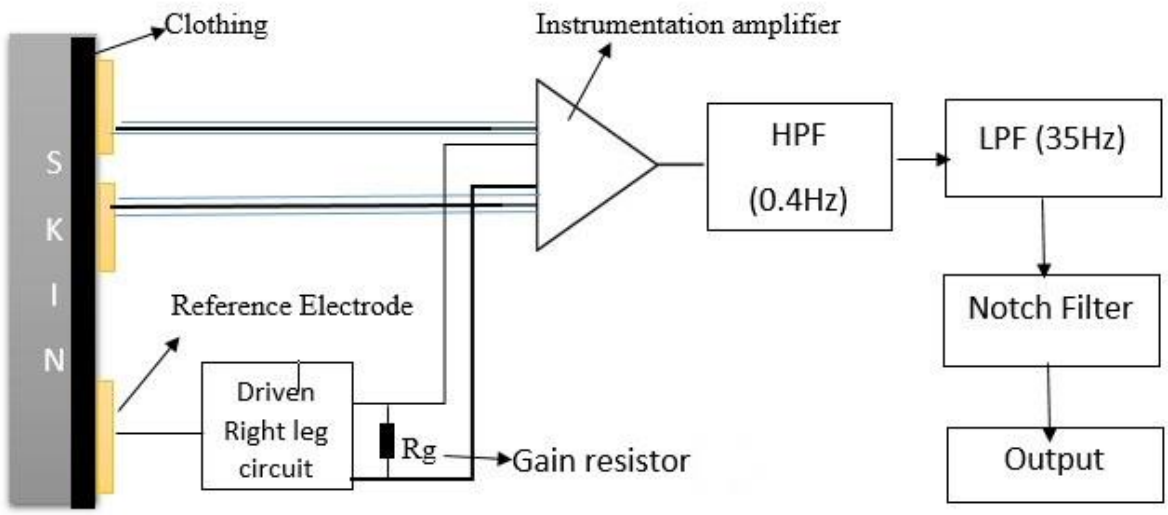

Fig. 5.3 Functional block diagram

As the figure explains, it is a three-electrode capacitive ECG sensing system. The output voltage signal after the filtering stage is acquired by means of myDAQ data acquisition system and further processing is done using the LabVIEW environment.

Fig. 5.4 Experimental setup

Two configurations of reference electrodes were tested. In the first configuration the reference electrode was connected in the lap belt. In the second configuration the reference electrode was the copper plate positioned under the occupant's right thigh. No appreciable difference between the two in terms of the quality of ECG recording was observed.

5.2 Virtual instrumentation

The flow chart depicted in the next page shows the entire procedure involved- right from acquiring signals to performing HRV evaluation.

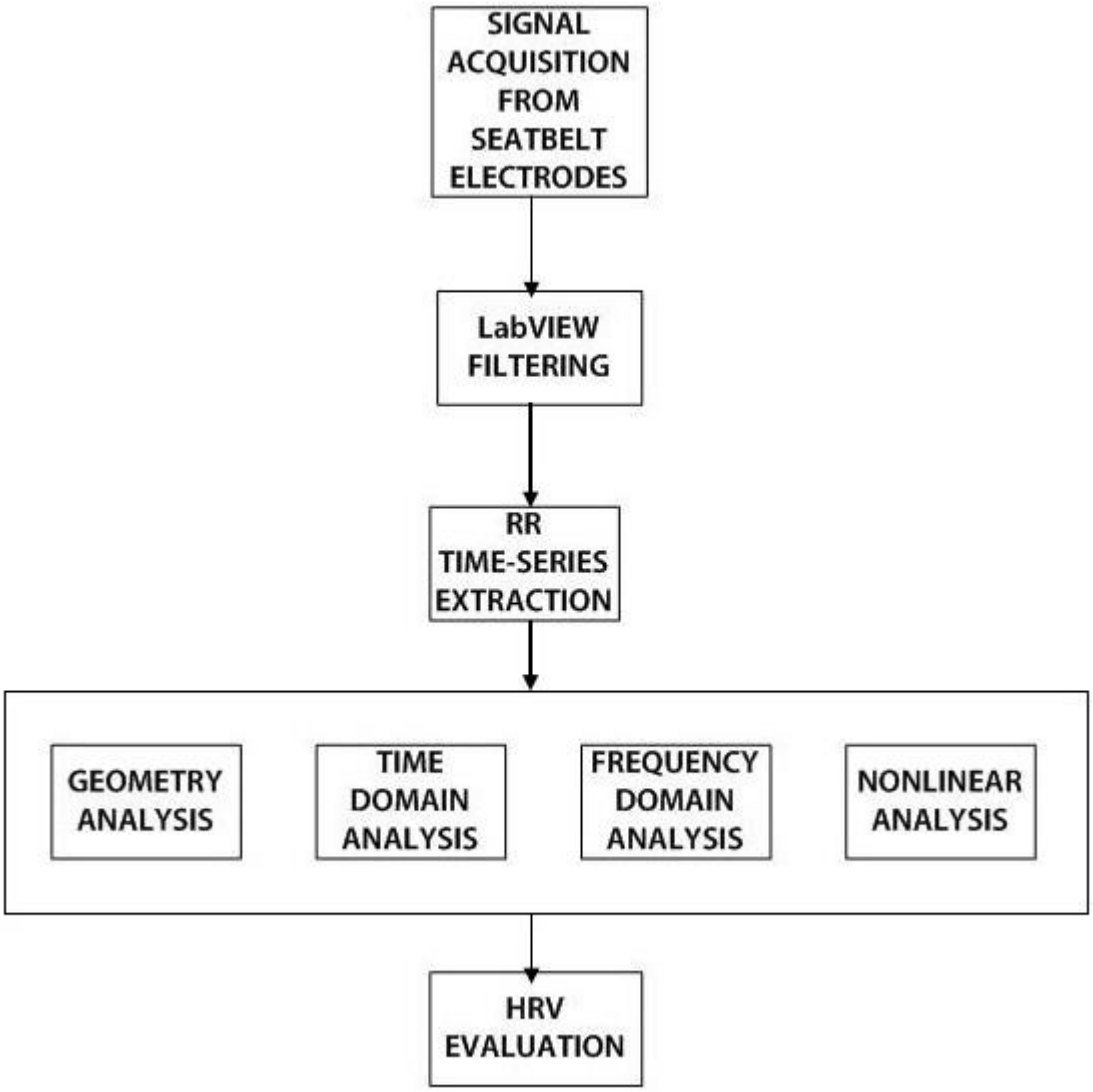

The LabVIEW 2013 software suite was used to acquire real-time ECG data via the USB port. Additionally, the 'biomedical toolkit 2013' was used to perform dedicated HRV computations such as the non-linear and frequency domain analyses. As opposed to the conventional programming using the written code, LabVIEW allows the user to build blocks, connect them to perform a desired task. Hence this type of programming is referred to as 'Data-flow' programming. Here 'data flow' determines the program execution routine. LabVIEW programs are called virtual instrumentation or VI is as their appearance and operation resembles that of physical instruments besides mimicking their functions. The LABVIEW has set of virtual instruments like oscilloscope, impedance analyzer, bode analyzer etc. It also lets the user to build custom VIs and save them as 'sub-VIs' to be used anywhere in the code. A typical LabVIEW program contains two components: a Front panel which can accept inputs from the

used and can double as a graph viewer; and a Block diagram which is where the graphical programming takes place.

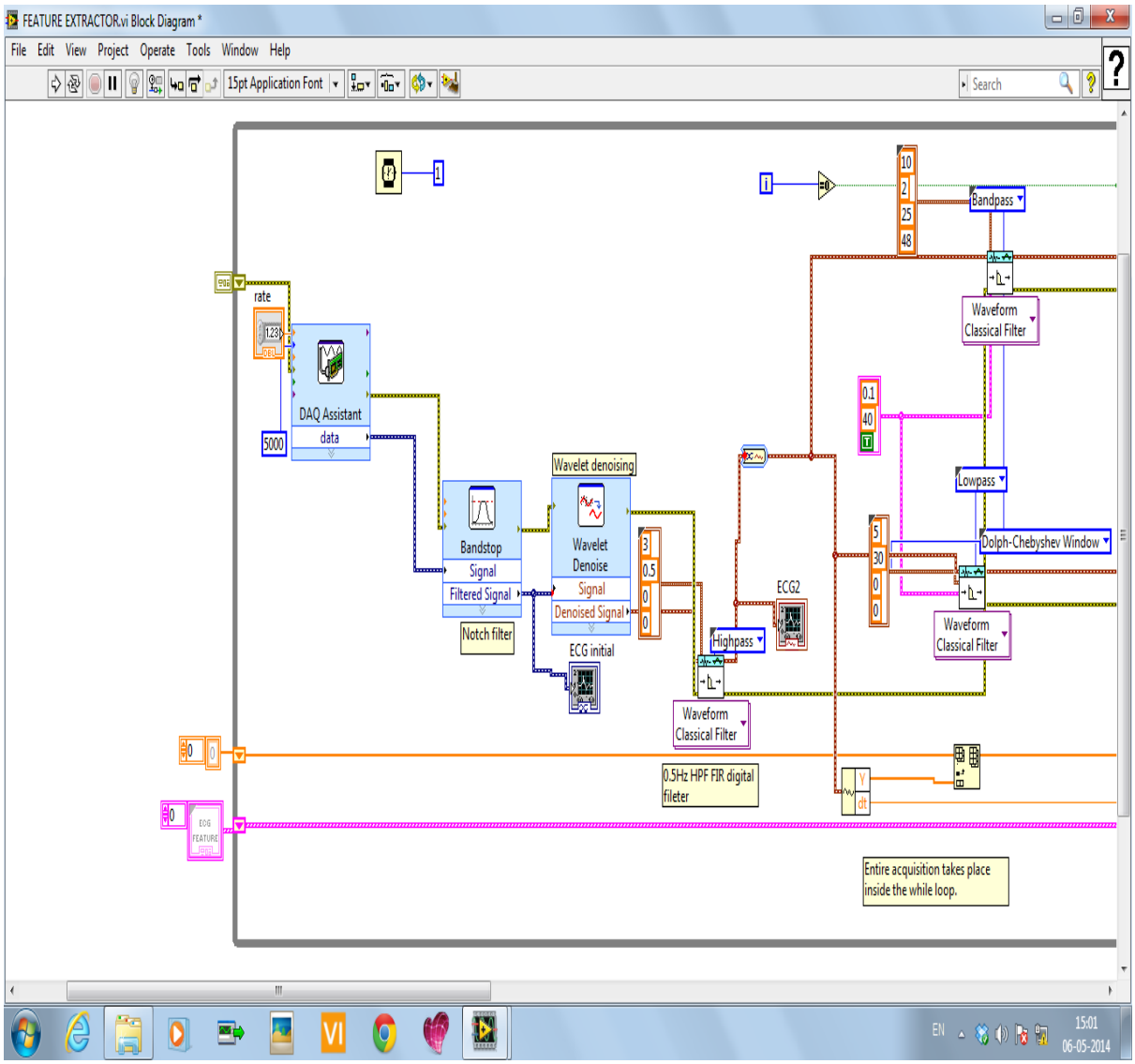

Fig. 5.5.1 Block diagram developed to perform HRV

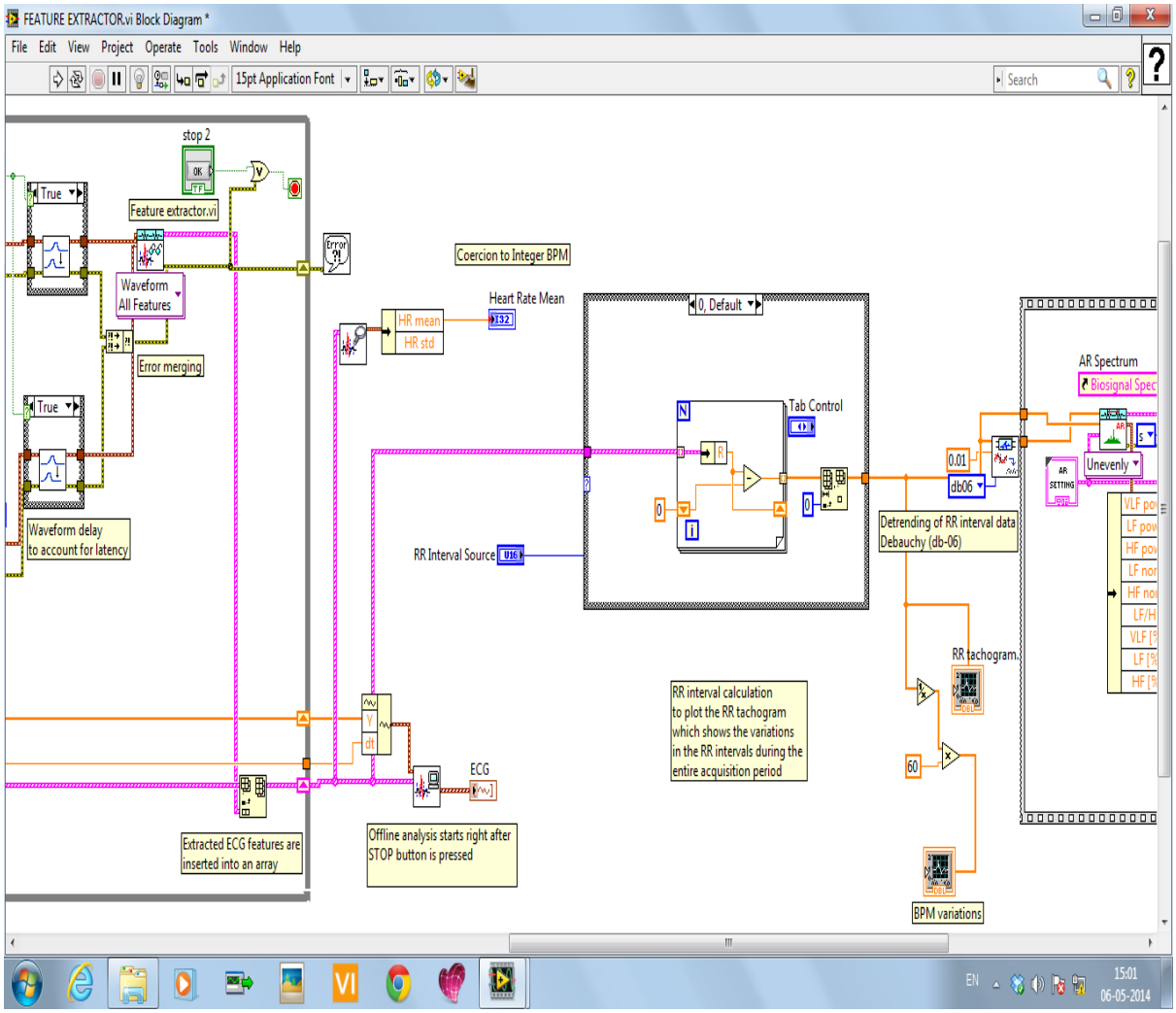

Fig. 5.5.2 block diagram continued

The ECG signal output is acquired from the signal processing unit at a sampling rate of 1000Hz. The signal has to undergo few more stages of signal processing before being used for the calculation of heart rate, and consequently the heart rate variability of the occupant. All the additional filtering is realized using LabVIEW. A notch filter is connected in order to remove any power line interference. Furthermore, the baseline wandering of the ECG is removed by connecting an FIR high-pass digital filter of 0.5Hz cut-off frequency in the block diagram. The baseline wander (BW) is basically noise whose components oscillate between 0.15 and 0.3 Hz. It results from respiration [19]. It is commonly caused by changes in electrode-skin impedance.

Figure 5.6.1 shows the ECG with baseline wandering. Whereas the figure 5.6.2 shows the same ECG without the baseline wandering by using a 0.5Hz FIR High-pass digital filter

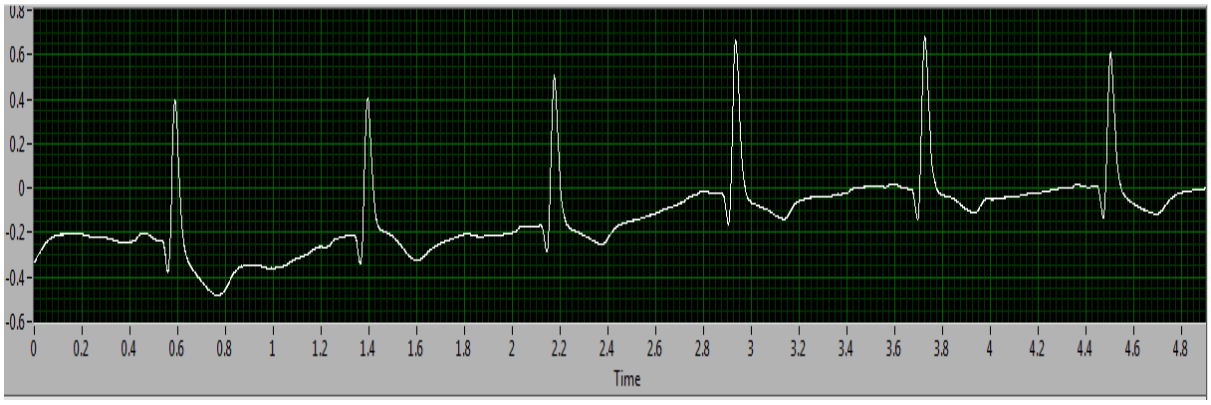

Fig.5.6.1 ECG with baseline wandering

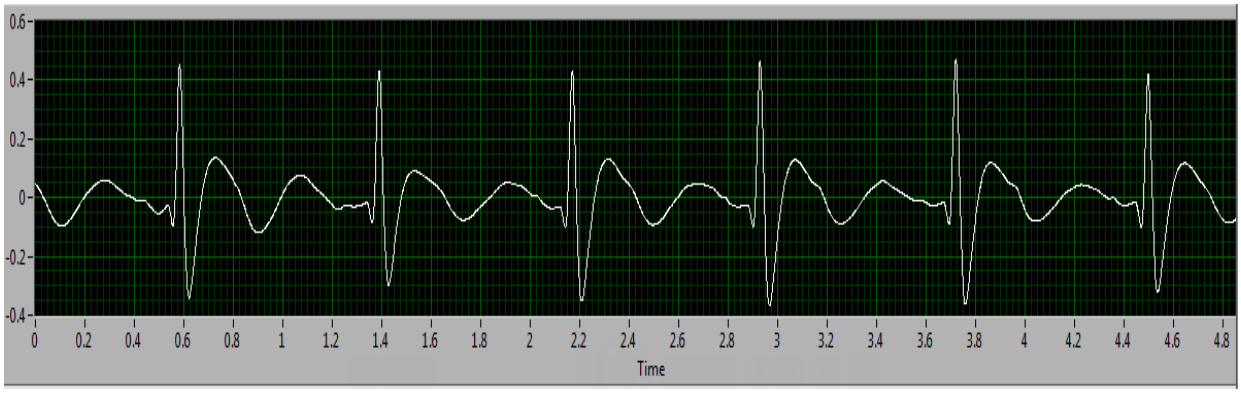

Fig. 5.6.2 ECG without Baseline wandering.

After removing the baseline wandering the resulting ECG signal is more stationary and explicit. However it still needs to be free from other wide band noise components which can be inevitable during a non-contact ECG recording. So wavelet de-noising is performed using the ‘wavelet de-noising’ VI to remove the noise. In order to make the QRS detection easier, an additional 10-25Hz band pass filter is used. This causes a latency in the signal. This delay can thus be removed by a ‘waveform delay’ VI. The function of this VI is to discard the first N/2 points of the first block of filtered ECG signal, where N equals to the order of the filter.

The next step after feature extraction is to build the RR interval array. It can be simply achieved by subtracting adjacent R positions as shown in the figure 5.7 by using a simple for loop.

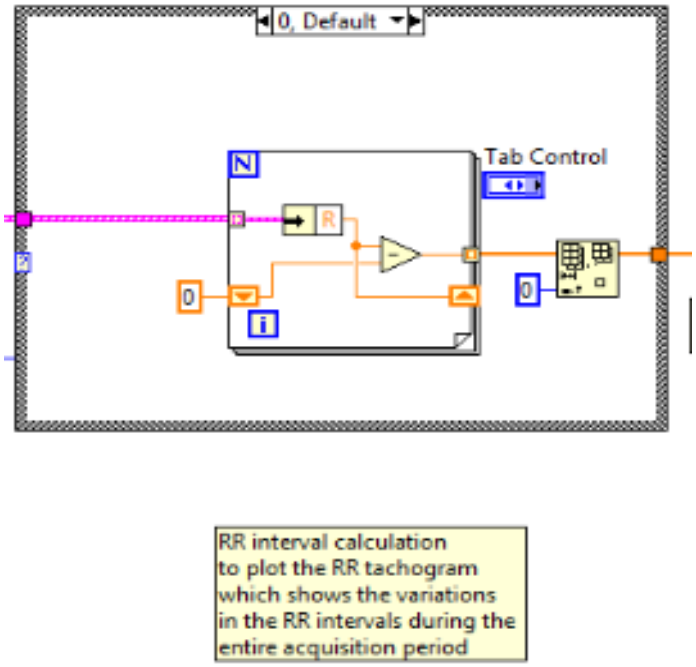

Fig. 5.7 RR interval calculation

5.3 Time domain HRV calculations

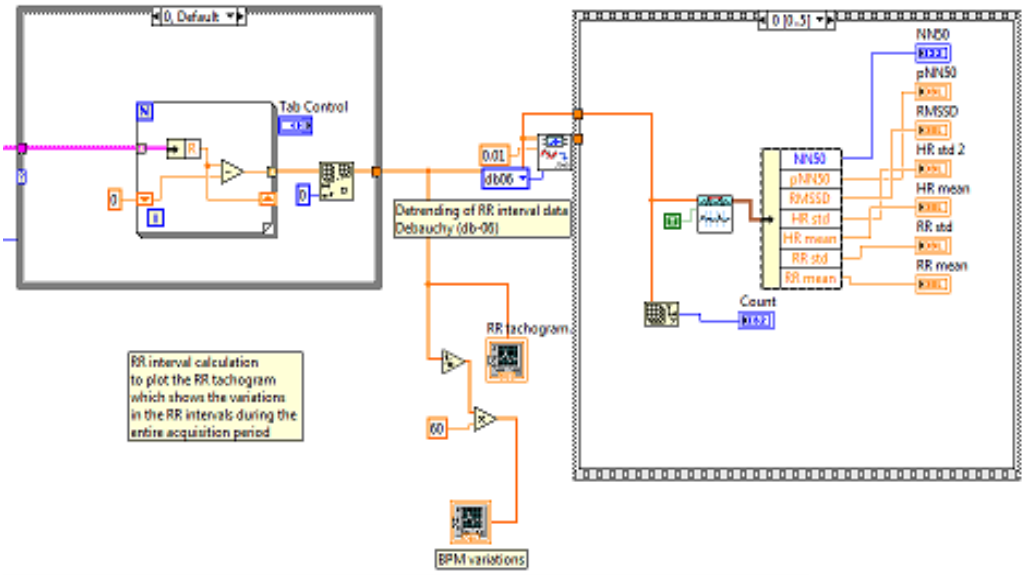

Fig. 5.8 shows time domain components calculation.

After the RR interval array is formed, it is plotted on a graph. This graph is the RR tachogram or in other words, RR time series. This time series is de-trended [20] prior to performing time domain HRV analysis in order to remove any abnormal/anomalous values. The heart-rate variations over the entire acquisition period are also plotted as shown in the block diagram in the fig. 5.3.

The result of this block diagram are the various time domain metrics that quantify heart rate variability. These include,

- NN50
- pNN50
- RMSSD
- HR (Standard deviation)
- HR (mean)
- RR interval length (mean)
- RR interval length (Standard deviation)

The above parameters are calculated from the sub-VI detailed below. The necessary algorithm and the related flow chart have been presented in the following section.

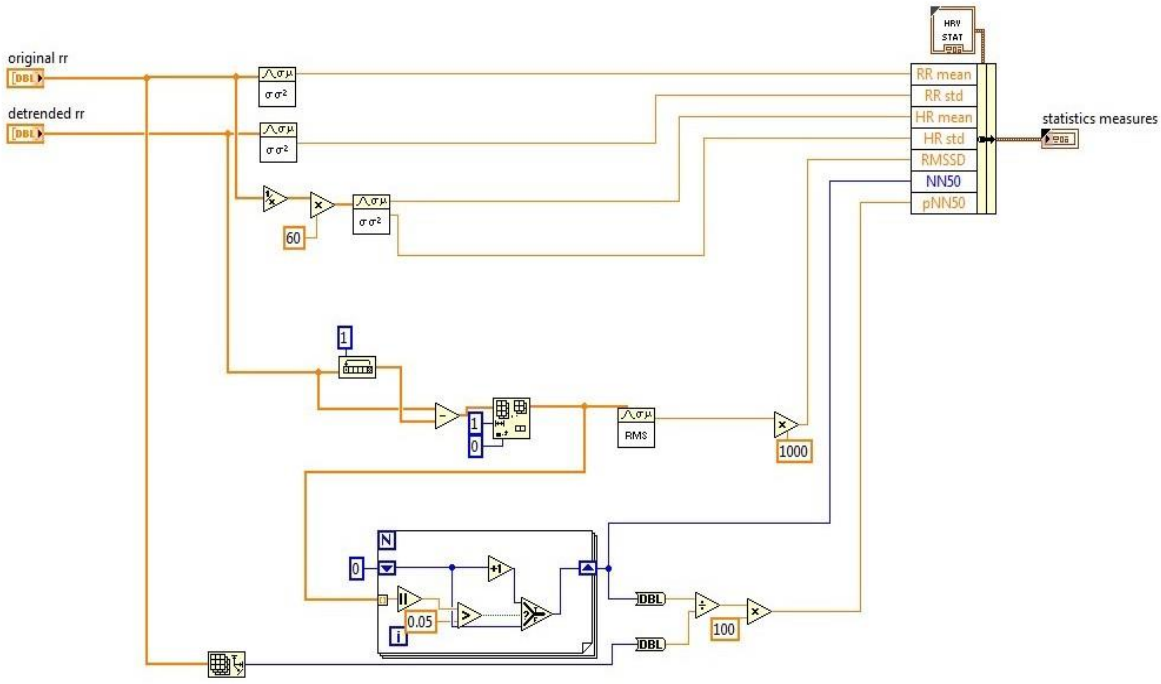

Fig. 5.8.1 shows the Sub-VI for calculating time domain HRV components.

5.3.1 The algorithm and flow chart for time domain HRV analysis.

Step 1: Remove any trends found in the RR tachogram and this 'Detrended' RR histogram is then passed on to the RMS/Mean block where the Mean RR interval and the standard deviation are calculated. Simultaneously, from the raw RR data calculate the heart rate of the entire tachogram by reciprocating the RR signal and multiplying it by 60. This array containing the BPM data is then passed on to the RMS/Mean block to compute the mean heart rate throughout the acquisition period.

Step 2: Find the size of the raw RR array and store it as 'Count'.

Step 3: Rotate the de-trended RR array left and subtract it from the original de-trended array.

Step 4: Delete the first element from the resulting array in order to eliminate any erroneous calculations. This array of data is then used to calculate the RMSSD

Step5: The same array is then converted into the absolute value. Initialize NN50=0.

Step 6: Compare the absolute value in the array with a constant-0.05. If greater than 0.05, NN50 is incremented. If not, the next absolute value in the array is compared with 0.05.

Step 7: Return NN50 value. And display the same.

Step 8: Divide NN50 value with the 'Count' obtained from Step 2, and multiply the resulting value with 100 to obtain pNN50 value.

The flowchart for calculating the time domain HRV indices is shown in the next page

(See Figure 5.8.2)

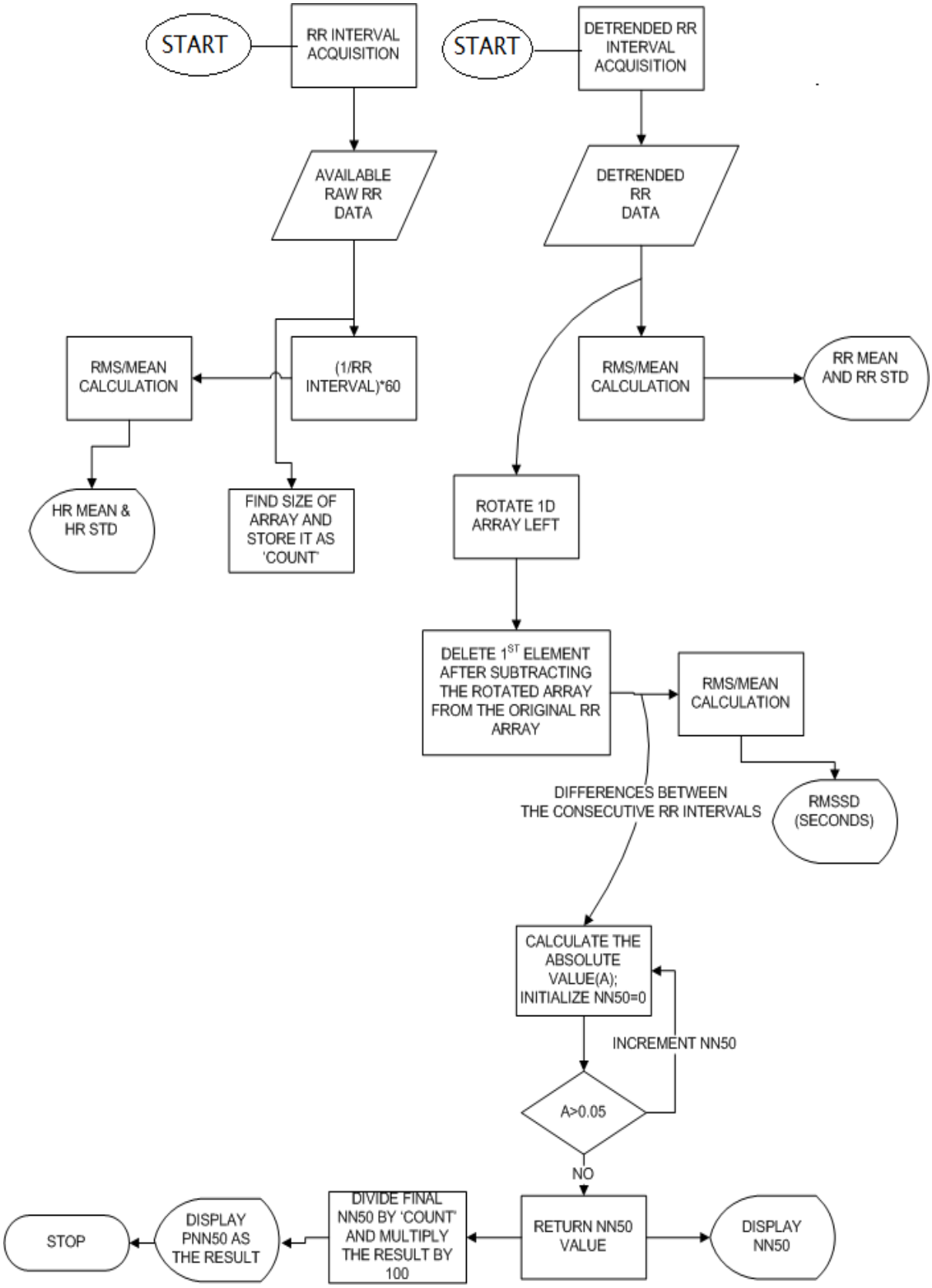

Fig 5.8.2 Flowchart to extract time-domain HRV metrics

5.4 Geometric and Nonlinear HRV methods

The VI for determining the heart rate variability using the geometric methods (Histogram) and the nonlinear methods are detailed in this section.

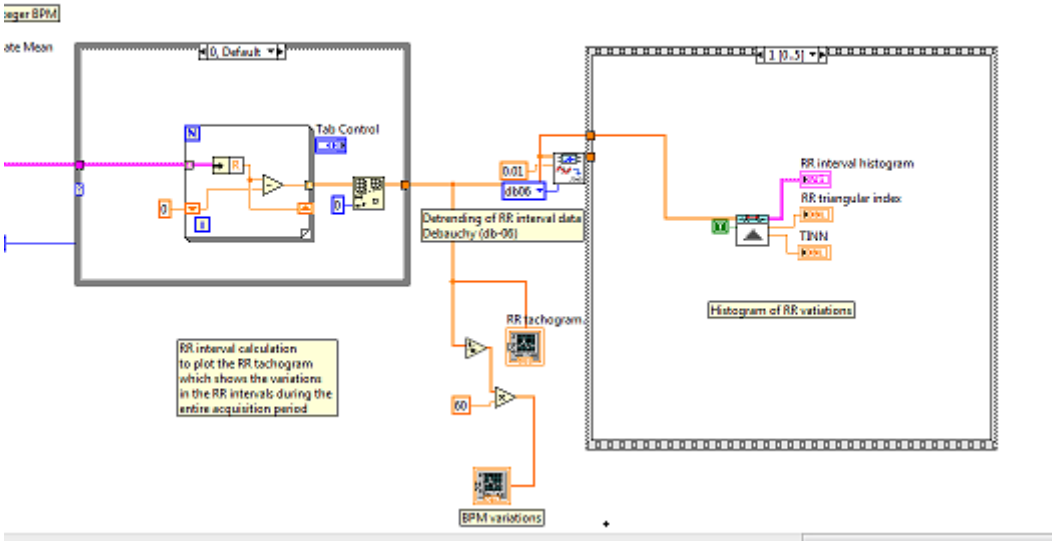

Fig 5.9 Block diagram for calculating the RR triangular index and the TINN.

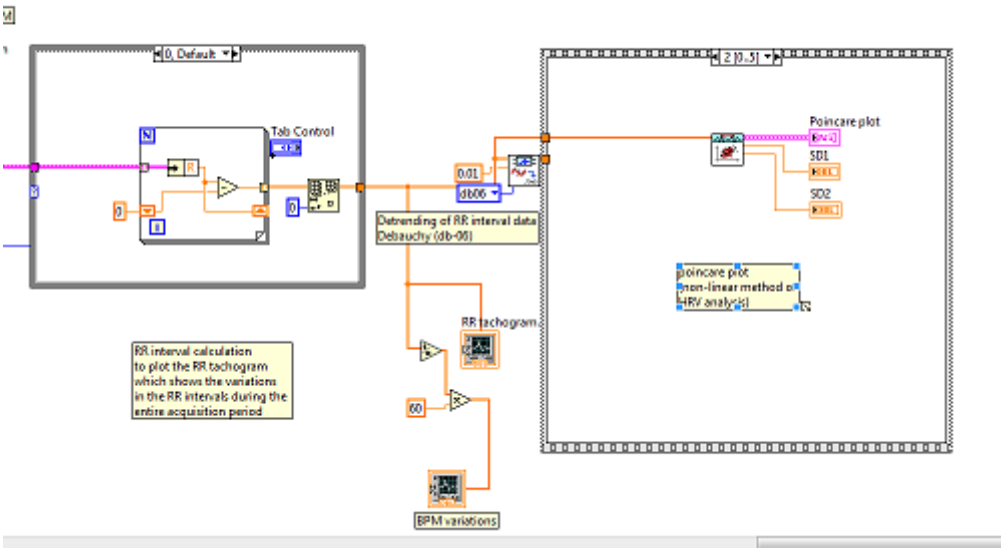

Fig 5.10 Block diagram using the 'Poincaré plot' VI

The standard deviations SD1 and SD2 are calculated from the block diagram shown in the fig. 5.10 which forms basis to quantify HRV using nonlinear methods.

5.5 Frequency domain HRV measurement

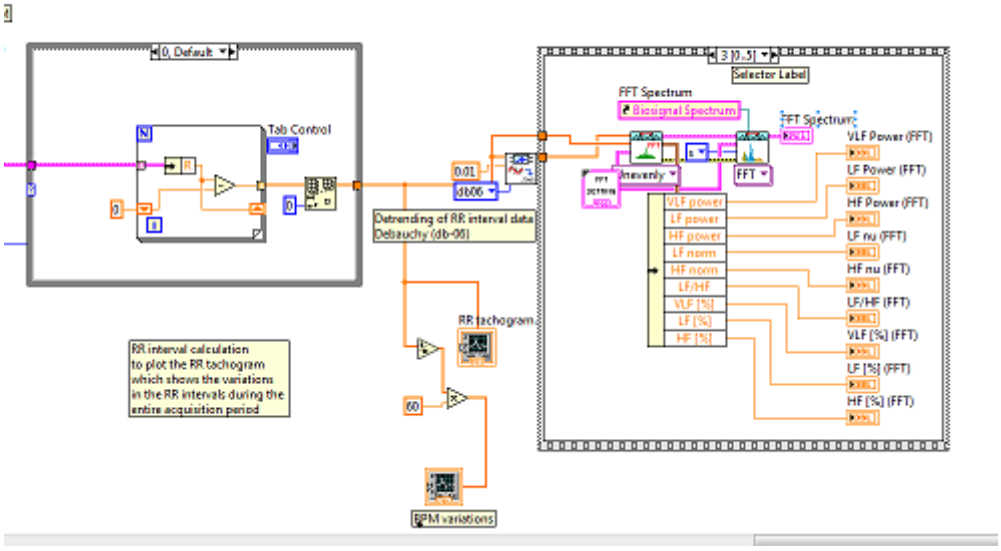

Fig. 5.11 shows FFT based HRV method

The FFT block requires both the raw RR data and the de-trended RR tachogram at a sampling frequency of 128 Hz (bin length of 0.0071825 seconds). The appropriate frequency ranges are given as inputs to the FFT block. FFT is performed on the RR time series and the power spectral density is plotted versus frequency. The power of a signal is the variance (square of the standard deviation) and hence the power spectral density (measured in milliseconds squared/frequency) vs. frequency graph is plotted. This is where LF power and HF power are calculated and the ratio LF/HF, which is a determinant of the sympathovagal balance is also displayed here.

Another approach to finding the frequency domain HRV parameters is the auto-regressive model which also helps in plotting the power spectral density graph. Here, too, the bin length of 7.1825ms is used. It is worthwhile to note that there are two peaks in the PSD graph. The lower frequency peak frequency is a measure of BP variations, while the higher frequency peak frequency is a measure of respiration rate.

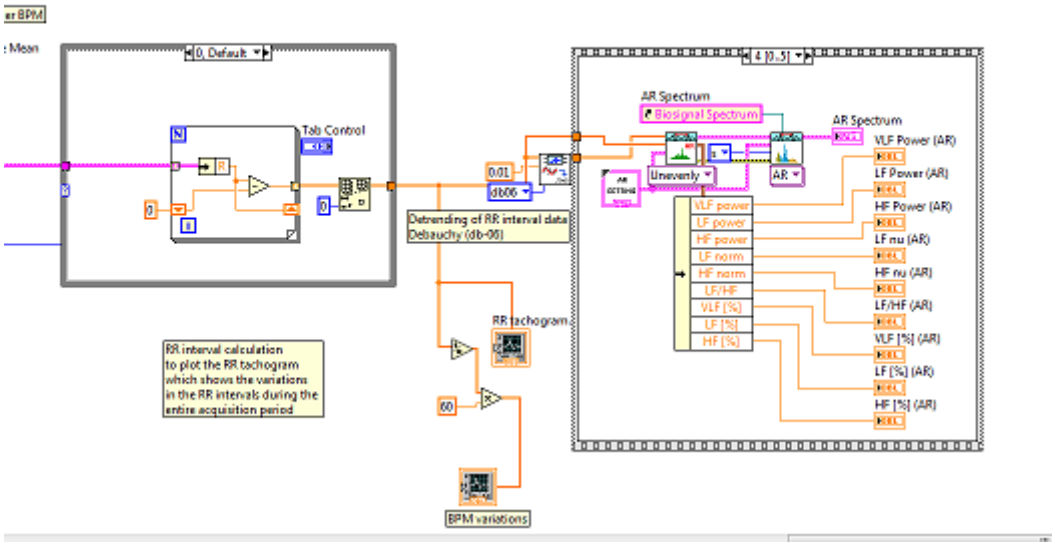

Fig. 5.12 block diagram to plot the AR Power spectrum

5.6 Results

Six healthy male volunteers with ages ranging from 22 to 35 were asked to sit on the chair, wearing the seatbelt with the capacitive sensors while their ECG was recorded for a period not less than 5 minutes as recommended by [8].

Fig. 5.13 shows a volunteer whose ECG is being recorded

All the necessary time domain and frequency domain readings are tabulated for all the volunteers. It was inferred that people with the RMSSD value in the range to 50-100ms are considered to have a moderately depressed HRV while those with the RMSSD value less than 50ms are said to have a highly depressed HRV.

Age (Years)	**HR**(mean) (bpm)	**HR**(std.dev.) (bpm)	**RMSSD** (ms)	**NN50**	**pNN50** (%)	**LF/HF** (AR)	**LF/HF** (FFT)
22	79.5	5	27.7	20	5.70	3.0	2.8
23	78	5	34.9	49	14.04	2.1	2.2
24	78	2.6	191.3	237	43.24	0.87	0.88
25	76	4.3	116.9	79	25.07	0.56	0.66
26	75	15.4	53.49	58	14.75	1.0	1.5
35	83	2.3	11.58	0	0	1.1	1.0

Table 5.1 shows HRV indices for all the subjects

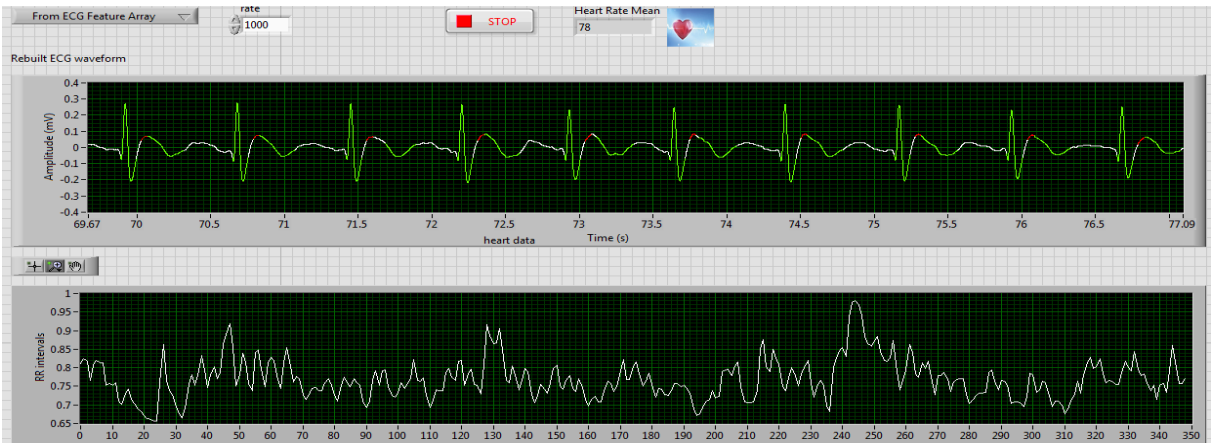

Fig. 5.14 ECG and RR tachogram of a 23 year old subject

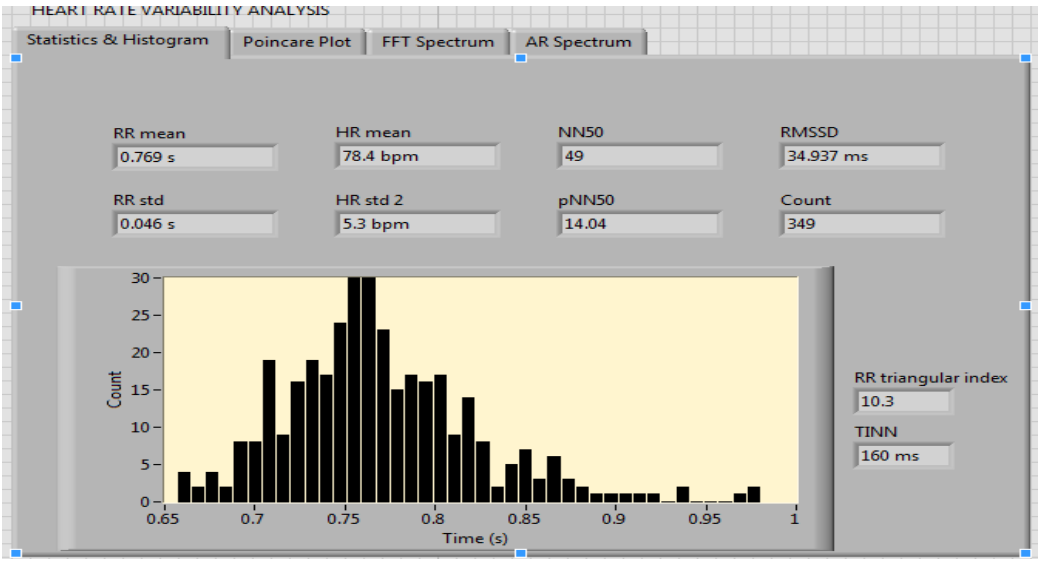

Fig. 5.15 Statistical HRV analysis

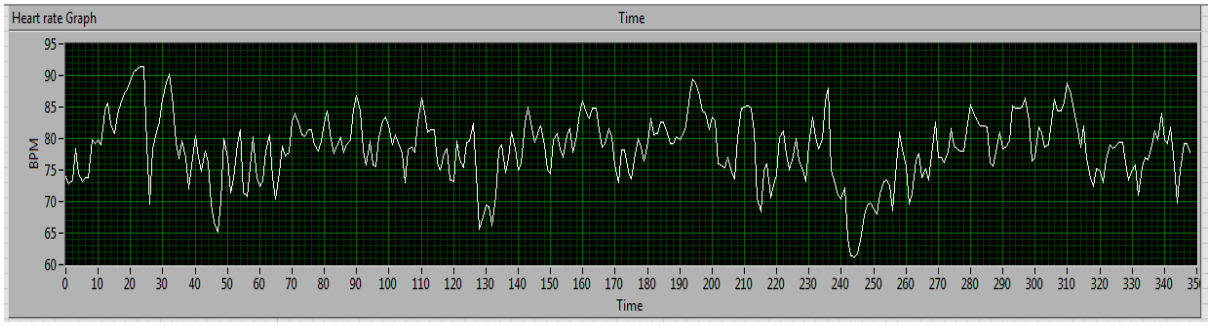

Fig.5.16 shows the heart rate (BPM) variations

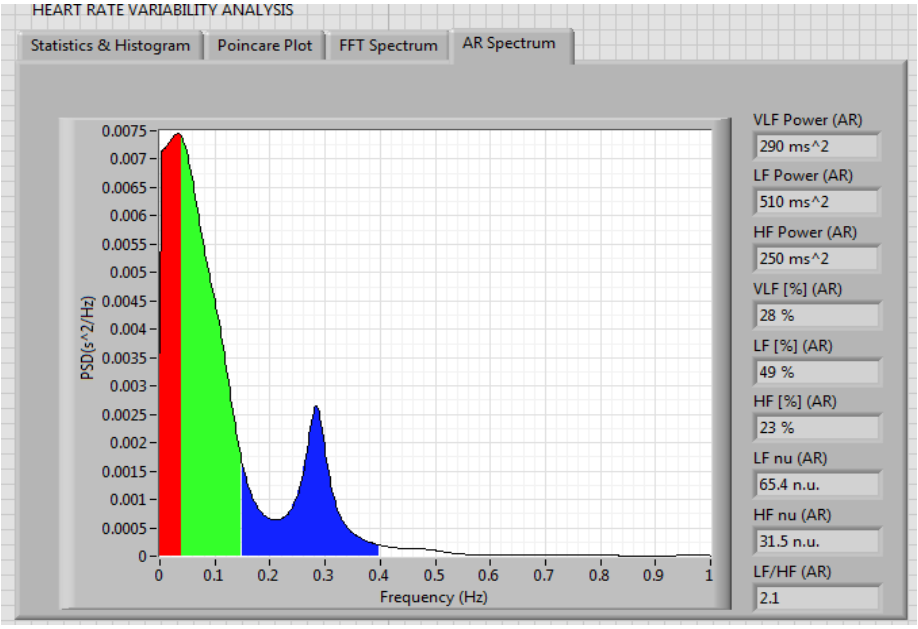

Fig. 5.17 AR power density spectrum of the 23 year old subject

The second peak at 0.26 Hz shows the respiration rate in (rpm) which is found to be 15.6rpm for this 23 year old male. His HR variations are plotted as shown in the figure 5.11

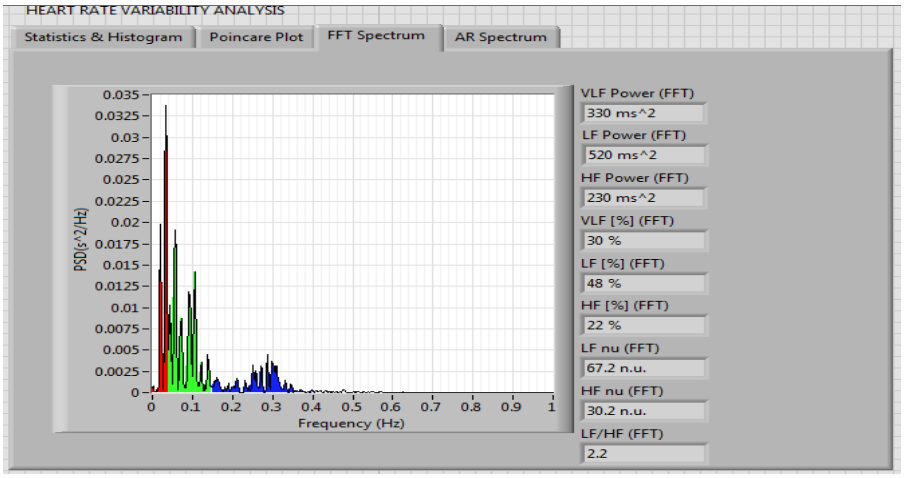

Fig. 5.18 FF HRV spectrum

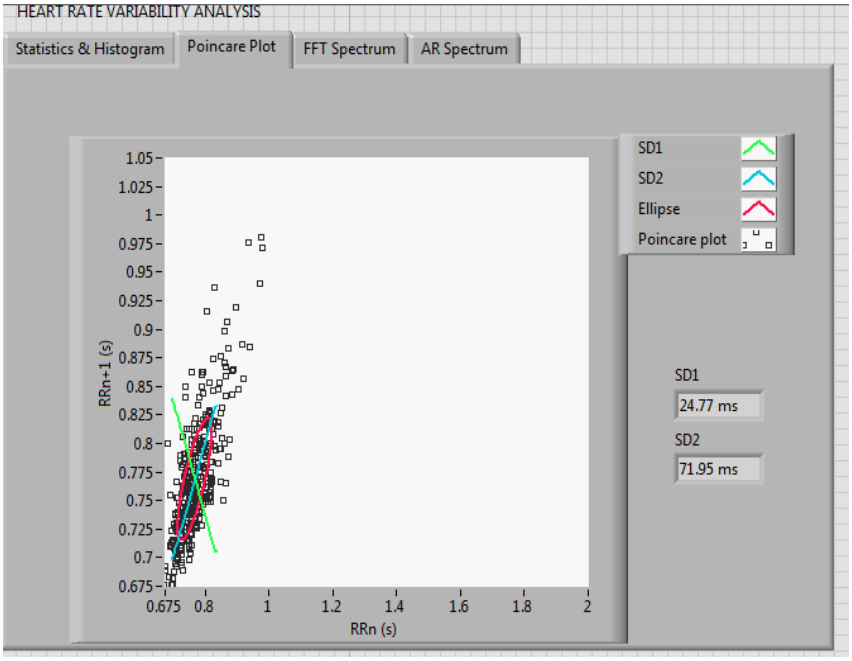

Fig.5.19 Poincare plot

The LF/HF ratio was roughly 2 which indicates a decrease in the parasympathetic activity during the acquisition period. However, a lower RMSSD of 35ms indicates that the HRV is moderately depressed in this individual.

Similar results for the 35 year old male volunteer are also presented here to better understand the change of HRV components with age.

Fig. 5.20 ECG RR tachogram of the 35 year old subject.

In the fig. 5.20, the ECG and corresponding RR intervals of a 35 year old subject are shown. It is to be noted that the X-axes for both the graphs are different. For the purpose of clarity, the ECG is shown magnified so as to cover only a few beat-intervals in the scale.

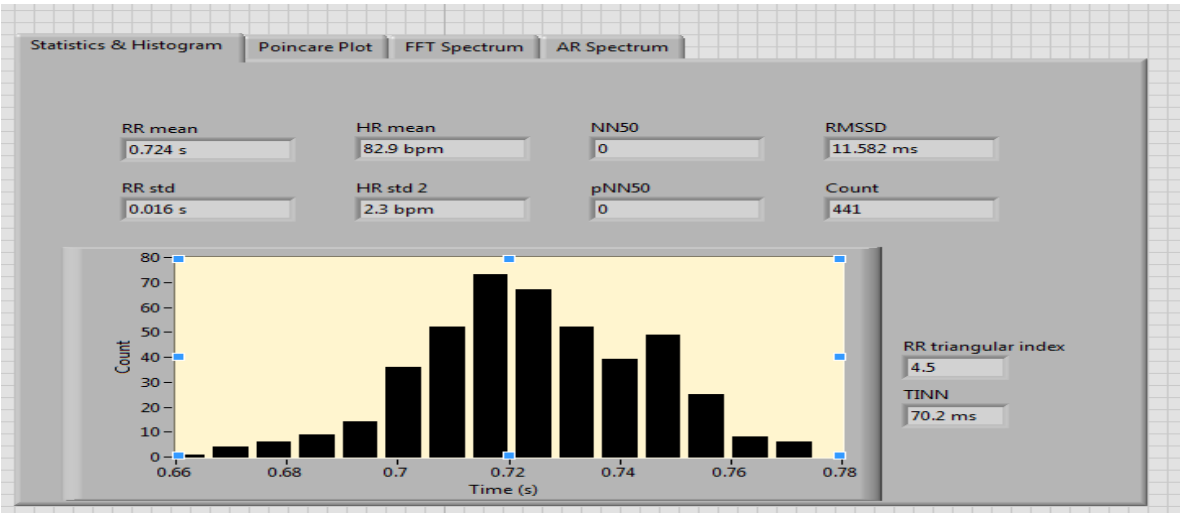

Fig. 5.21 Statistical HRV components of the 35 year old subject

The RMSSD was found to be about 12ms which indicates a highly depressed HRV. As expected, the NN50 and hence the pNN50 values are negligible in this individual which also indicates that the HRV is very low in this individual.

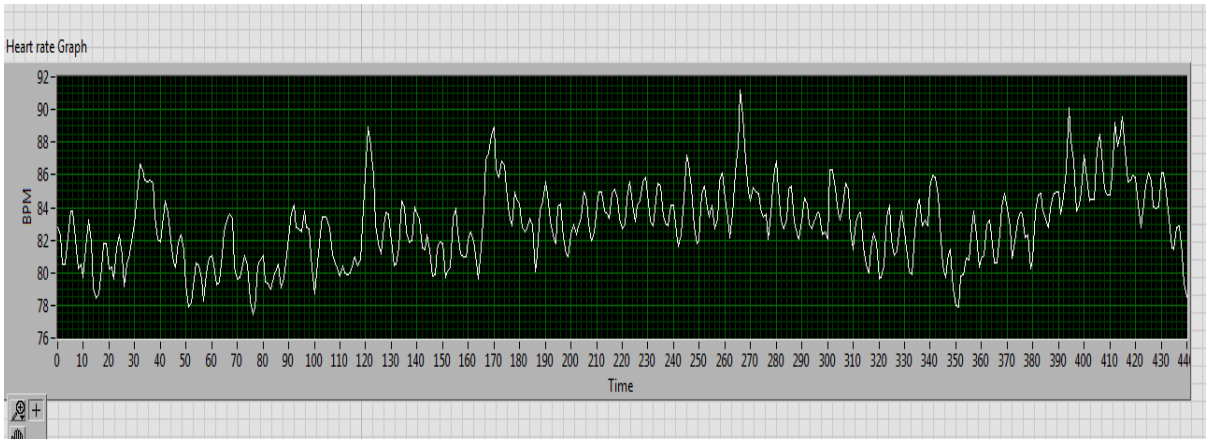

Fig. 5.22 shows HR (BPM) variations

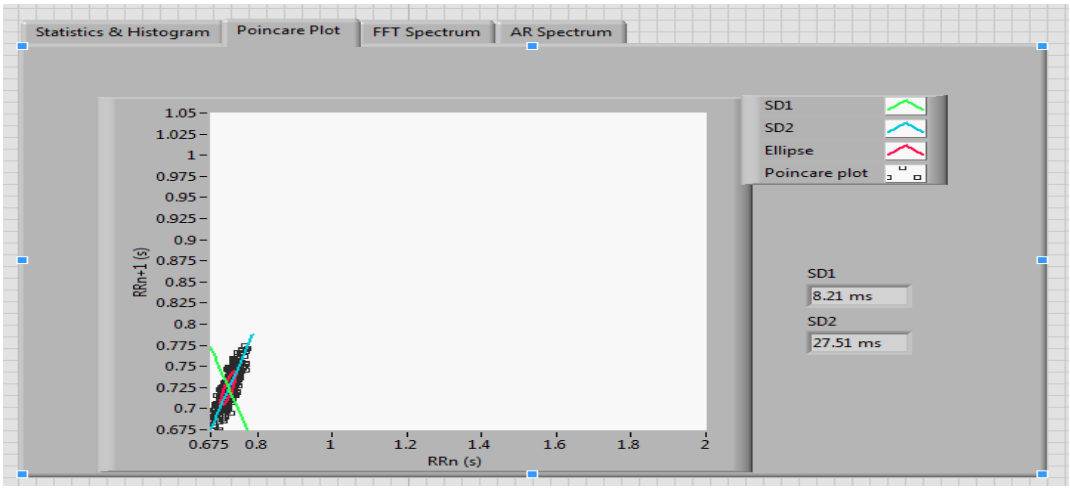

Fig. 5.23 depicts the Poincare plot

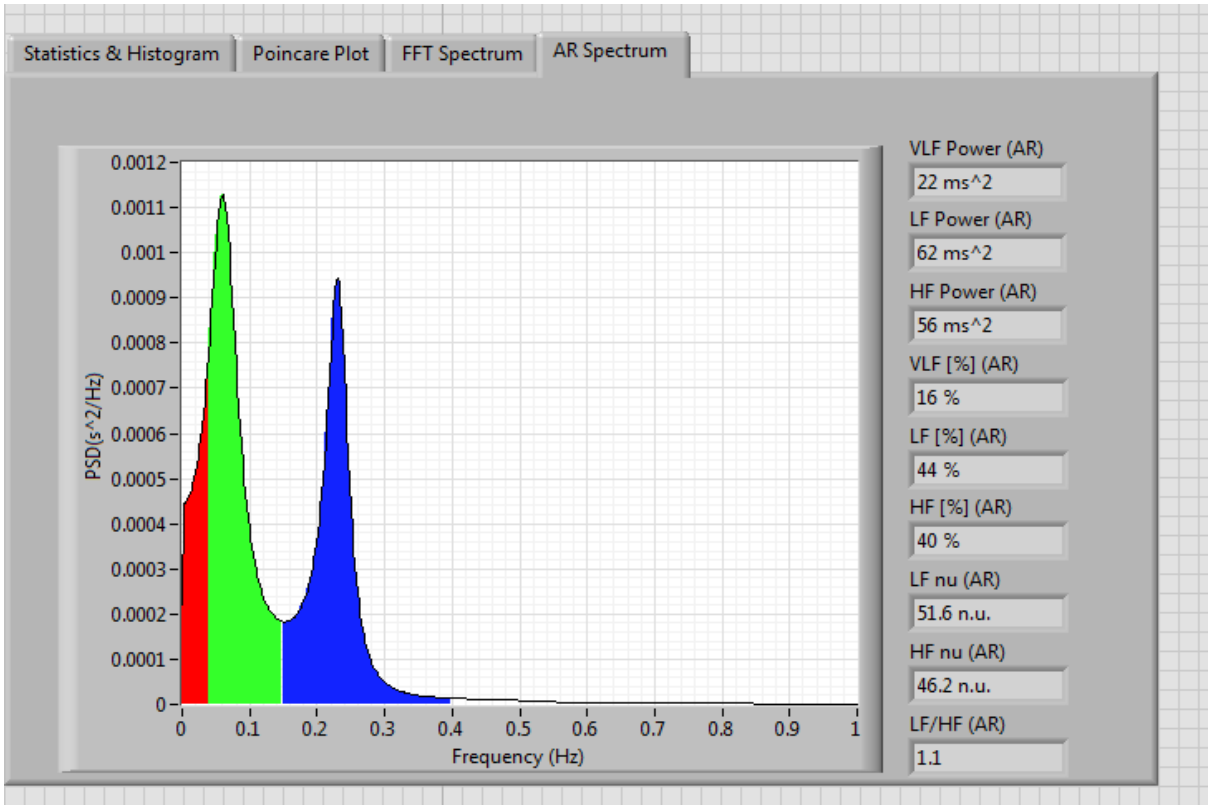

5.24 shows AR spectrum

Fig. 5.24 shows the PSD with modelled using auto-regression analysis. The AR model specifies that the output variable depends linearly on its own previous values.

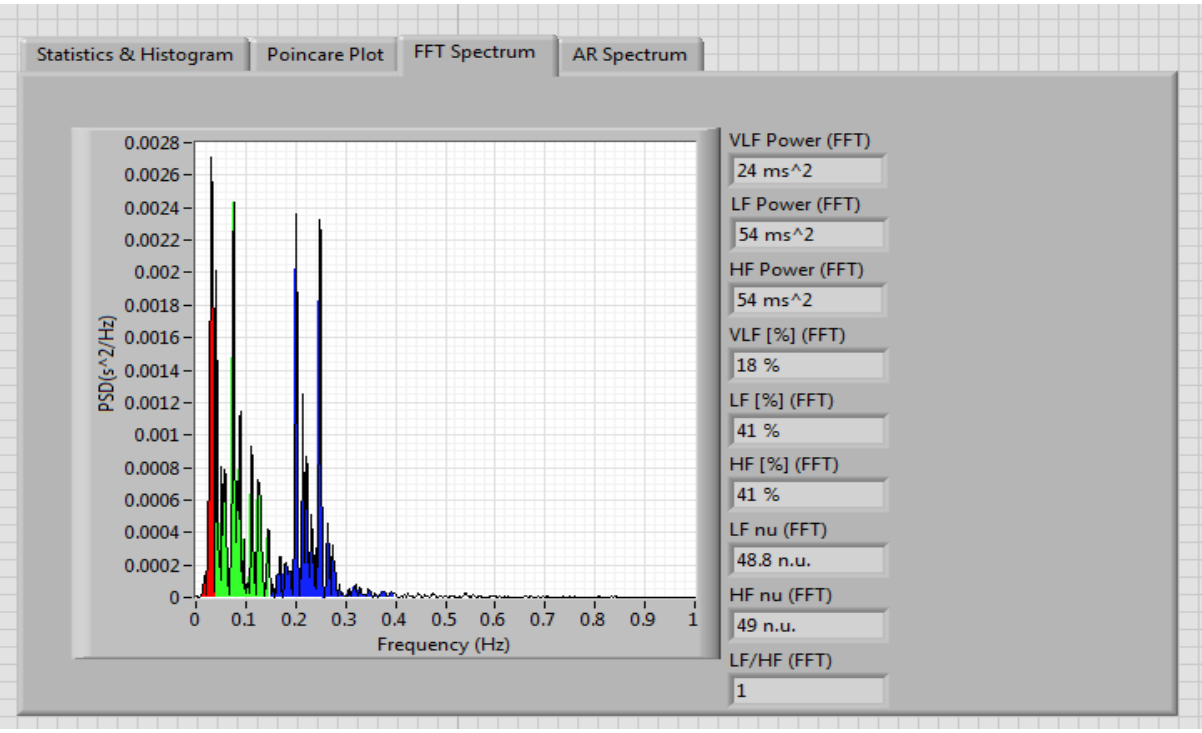

Fig. 5.25 shows the FFT HRV spectrum

The LF/HF ratio is 1 which indicates the sympathetic and parasympathetic stimuli are acting on the SA node in equal proportions. Furthermore, the high frequency peak found at 0.23Hz indicates the respiration rate as 13.8rpm.

5.7 Conclusions

From the feasibility study and the results thus obtained, the following inferences can be drawn:

- The setup provided better capacitive coupling and, thereby better ECG recording and better insights into a person's HRV evaluation only when he is wearing a single layered clothing (such as a t-shirt) rather than a shirt having a pocket (this creates two layers thereby distorting the signal considerably).
- The capacitive coupling was almost negligible (indiscernible) when polyester material was used.
- For the setup, the two active electrodes were 12.5cm X 5 cm in dimensions while the reference electrode placed on the lap belt was of dimensions 27cm X 5cm which proved to be enough for a satisfactory recording of ECG, and consequently the HRV.
- It was also concluded that the HRV indices show a decreasing trend as the age advances. Furthermore, HRV was quite low in a person with low physical activity.

CHAPTER 6

CONCLUSIONS

6.1 Summary of the work

The work presented in the thesis aims to explore the feasibility of contact-free ECG measurement incorporated in the car's seat-belt. It has been observed that, for the two configurations mentioned in this thesis, ECG was satisfactorily recorded. Since the two electrodes which are placed on the shoulder harness (sash belt) were optimally placed so as to improve the capacitive coupling, the ECG recorded was almost like in a conventional contact ECG recording. The idea behind recording ECG from a car's seat belt was mainly aimed at ubiquitous heart rate monitoring of the driver who is prone to injury caused by an accident. The fact that the seat belt is continuously pressed against the occupant's clothing (and hence his body) has enormously influenced our idea of incorporating electrodes on the seat belt of a car. The signal quality was the best when cotton clothing was used. However, the capacitive coupling was negligible when polyester was used in out experiment. Since the setup could be placed within an automotive environment, it can be used to monitor the drowsiness of the driver.

Besides plotting the occupant's heart rate fluctuations over the entire acquisition time, his heart rate variation (HRV) analysis can also been carried out using this scheme. HRV measures qualitatively the amount of stress a person is in. It is also a non-invasive technique to detect SIDS in infants. The HRV can be a very useful tool in determining the influence of autonomic nervous system on the SA node (sinus rhythm) which in turn affects the heart rate. All the necessary tools for HRV analysis have been presented in this thesis.

Out of the time-domain HRV metrics RMSSD is the most important. Persons with the RMSSD value below 50ms, have a highly depressed HRV while those with the RMSSD value in the range 50ms-100ms are said to have a moderately depressed HRV. The RMSSD in a healthy individual is above 150ms. HRV decreases with age. It is observed to be low in people leading a sedentary lifestyle and very high in those who exercise regularly. Besides, the Time domain methods, the frequency domain methods to quantify HRV have also been presented in

the thesis. The LF/HF ratio determines the sympathovagal balance. The AR PSD spectrum provides valuable information about a person's respiration rate and BP fluctuations. However, these frequency domain tools are a part of an ongoing research. Nevertheless, the HRV still successfully provides valuable insights into a person's autonomic nervous system and its influence on the Sinus rhythm.

6.2 Future scope

The prototype can be effectively used to carry out all the necessary HRV analysis besides calculating the heart rate in an adult. The capacitive sensors can be appropriately designed to carry out cardiovascular monitoring of infants. In order to remove motion artefacts that distort ECG waveform, an array of electrodes can be placed in a chair and can be multiplexed so as to keep the signal intact even when the occupant shifts positions. A dedicated signal processing unit which works in conjunction with a monitor placed on the dashboard can be placed on the belt itself and the entire cardiovascular monitoring could take place by the 'telemetry' principle wherein the doctor can monitor the patient from a remote location.

REFERENCES

[1] R. M. Rangayyan, “Biomedical Signal Analysis”—a case study approach, IEEE press series in Biomedical Engineering, 2002.

[2] D. Obeid, S. Sadek, G. Zaharia, and G. El Zein, “Multitunable microwave system for touchless heartbeat detection and heart rate variability extraction,” Microw. Opt. Technol. Lett., vol. 52, no. 1, pp. 192–198, 2010

[3] Jure Kranjec “Novel Methods for Noncontact Heart Rate Measurement: A Feasibility Study”IEEE TRANSACTIONS ON INSTRUMENTATION AND MEASUREMENT, VOL. 63, NO. 4, APRIL 2014

[4] A. E. Mahdi and L. Faggion, “Non-contact biopotential sensor for remote human detection,” J. Phys., Conf. Ser., vol. 307, no. 1, p. 012056, 2011.

[5] R. J. Prance, S. T. Beardsmore-Rust, P. Watson, C. J. Harland, and H. Prance, “Remote detection of human electrophysiological signals using electric potential sensors,” Appl. Phys. Lett., vol. 93, no. 3, pp. 033906-1–033906-3, 2008

[6] Nickel, P.; F. Nachreiner (2003). "Sensitivity and Diagnostics of the 0.1-Hz Component of Heart Rate Variability as an Indicator of Mental Workload". Human Factors 45 (4): 575–590.

[7] Jönsson, P. (2007). "Respiratory sinus arrhythmia as a function of state anxiety in healthy individuals". International Journal of Psycho-physiology 63 (1): 48–54

[8] “Heart rate variability Standards of measurement, physiological interpretation, and clinical use” European Heart Journal (1996) 17, 354–381

[9] Time Domain Measurements of Heart Rate Variability, In: Malik M., Camm A.J. (eds.): Heart Rate Variability, Armonk, N.Y. Futura Pub. Co. Inc., pp 33-45, 1995

[10] Umetani K “Twenty-four hour time domain heart rate variability and heart rate: relations to age and gender over nine decades.” J Am Coll Cardiol. 1998 Mar 1; 31(3):593-601.

[11] “Decrease in heart rate variability with overtraining: assessment by the Poincaré plot analysis.” Mourot L Clin Physiol Funct Imaging. 2004 Jan;24(1):10-8.

[12] Sayers (1973). "Analysis of Heart Rate Variability". Ergonomics 16 (1): 17–32.

[13] Eckberg D.L.: Sympathovagal Balance, Circulation, 96:3224-3232, 1997.

[14] Hirsch J.A., Bishop B.: Respiratory sinus arrhythmia in humans: how breathing pattern modulates the heart rate, Am. J. Physiol., 241:11620-11629, 1981

[15] Kamath M.V., Fallen E.L.: Power spectral analysis of HRV: a non-invasive signature of cardiac autonomic functions, Crit. Rev. Biomed. Eng. 21(3):245-311, 1993.

[16] “Signal Processing Methods For Heart Rate Variability”, GD Clifford DPhil. Thesis, Oxford University, Michaelmas 2002.

[17] Rosangela “Poincaré plot indexes of heart rate variability: Relationships with other nonlinear variables” Autonomic Neuroscience Volume 177, Issue 2, October 2013, Pages 271–274

[18] De Vito, G "Effects of central sympathetic inhibition on heart rate variability during steady-state exercise in healthy humans" Clinical Physiology and Functional Imaging Volume 22, Issue 1, 2002, Pages 32-38

[19] Manuel Blanco "ECG signal denoising and baseline wander correction based on the empirical mode decomposition" Computers in Biology and Medicine 38 (2008) 1 – 13

[20] W. Aziz, R. Abbas, and M. Arif, "Detrended fluctuation analysis of synthetic and real RR-interval time series of healthy subjects," J. Appl. Em. Sci, vol. 1, no. 2, pp. 58–63, 2005.

[21] AHAMMED MUNEER K V's thesis 'DESIGN AND DEVELOPMENT OF A NON-CONTACT ECG RECORDING INSTRUMENT FOR CONTINUOUS CARDIOVASCULAR MONITORING

CURRICULUM VITAE

Name	:	Guru Charan Teja Kallakuri
Date of birth	:	14th December 1990
Place of birth	:	Vijayawada, Andhra Pradesh
Education	:	B.Tech. from University College of engg., JNTU Kakinada, Kakinada, 2012 batch
Email	:	charan0329@icloud.com